iScience

CellPress
OPEN ACCESS

Article

The different impact of drug-resistant *Leishmania* on the transcription programs activated in neutrophils

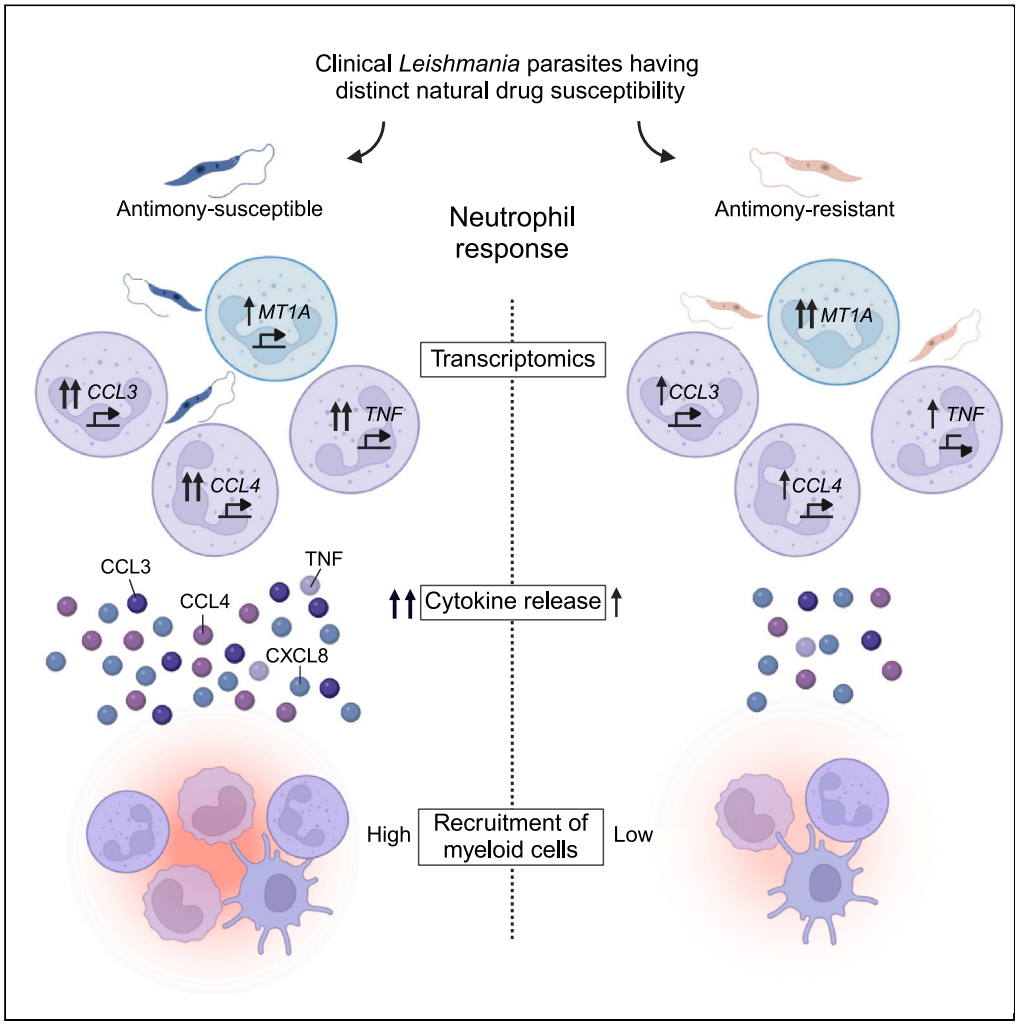

Míriam Díaz-Varela, Andrea Sanchez-Hidalgo, Sandra Calderon-Copete, ..., Olga Lucía Fernández, Nancy Gore Saravia, Fabienne Tacchini-Cottier

miriam.diazvarela@unil.ch (M.D.-V.)
fabienne.tacchini-cottier@unil.ch (F.T.-C.)

Highlights

Drug-resistant parasites induce distinct neutrophil transcriptional programs

Meglumine-antimoniate-resistant (MA^R) *Leishmania* limits neutrophil chemokine release

Infection with MA^R parasites impairs CCL3-driven early myeloid cell recruitment

Díaz-Varela et al., iScience *27*, 109773
May 17, 2024
https://doi.org/10.1016/j.isci.2024.109773

iScience

CellPress
OPEN ACCESS

Article

The different impact of drug-resistant *Leishmania* on the transcription programs activated in neutrophils

Míriam Díaz-Varela,[1,*] Andrea Sanchez-Hidalgo,[2,3] Sandra Calderon-Copete,[4] Virginie Tacchini,[1] Tobias R. Shipley,[1] Lady Giovanna Ramírez,[2,3] Julien Marquis,[4] Olga Lucía Fernández,[2,3] Nancy Gore Saravia,[2,3] and Fabienne Tacchini-Cottier[1,5,*]

SUMMARY

Drug resistance threatens the effective control of infections, including parasitic diseases such as leishmaniases. Neutrophils are essential players in antimicrobial control, but their role in drug-resistant infections is poorly understood. Here, we evaluated human neutrophil response to clinical parasite strains having distinct natural drug susceptibility. We found that *Leishmania* antimony drug resistance significantly altered the expression of neutrophil genes, some of them transcribed by specific neutrophil subsets. Infection with drug-resistant parasites increased the expression of detoxification pathways and reduced the production of cytokines. Among these, the chemokine CCL3 was predominantly impacted, which resulted in an impaired ability of neutrophils to attract myeloid cells. Moreover, decreased myeloid recruitment when CCL3 levels are reduced was confirmed by blocking CCL3 in a mouse model. Collectively, these findings reveal that the interplay between naturally drug-resistant parasites and neutrophils modulates the infected skin immune microenvironment, revealing a key role of neutrophils in drug resistance.

INTRODUCTION

Antimicrobial drug resistance (DR) poses a global threat to the effective treatment of infectious diseases. DR is a major challenge in assuring effective treatment of neglected tropical diseases (NTDs), which principally affect poor populations and rely on only a handful of drugs for their control.[1] Leishmaniases are NTDs caused by parasites of the genus *Leishmania*. They are the second largest cause of parasitic death after malaria. Pentavalent antimonial drugs such as meglumine antimoniate (MA) are the first line of antileishmanial treatment in most countries since the mid-20th century but there are increasing reports of treatment failure and evidence of resistance.[2,3] Due to the limited number of drugs with similar efficacy and availability,[4] multiple efforts have been undertaken to understand the basis of resistance to antimonial drugs and its relationship with treatment failure.[5,6] DR has mostly been studied following *in vitro* selection of drug-resistant populations, and only few studies have evaluated the drug susceptibility profile of circulating clinical strains of *Leishmania*.[3,7] Two subpopulations of *Leishmania (Viannia) panamensis*, distinguished by isoenzyme profiles defined as zymodemes, showed divergent susceptibility to antimonial drugs *in vitro*.[7] Naturally drug-resistant strains isolated from *Leishmania* patients provide the unique opportunity to discover parasite and host mechanisms converging *in vivo* to determine DR and treatment failure. As in other infectious diseases, DR in leishmaniasis has been traditionally assumed to be determined by the causative pathogen. However, DR and treatment failure are now recognized to be multifactorial. Increasing evidence suggests that the immune status of the host can significantly impact therapeutic responses in leishmaniasis.[8–10] Although DR and host immunity are critical factors in the outcome of infections, their complex interactions remain largely unknown.

Neutrophils, the predominant leukocytes in human circulation, play a pivotal role in the host response to *Leishmania* infection, promoting either protective or detrimental immune responses.[11] Neutrophils can prevent pathogen dissemination by a plethora of effector functions, including release of reactive oxygen species (ROS) and neutrophil extracellular traps.[12,13] Neutrophils are among the first immune cells recruited to the site of infection, and their rapid cytokine release is essential to orchestrate innate and adaptive immunity.[14,15] However, many *Leishmania* spp. have evolved mechanisms to escape neutrophil killing.[16] Moreover, dysregulated activation of neutrophils might lead to excessive inflammation and damage to the host tissue. Despite the importance of neutrophils in leishmaniasis, their role in infections with *Leishmania* parasites of divergent drug susceptibility has not been addressed until recently. *Ex vivo* assays showed that human

[1]Department of Immunobiology, WHO Collaborative Center for Research and Training in Immunology, University of Lausanne, 1066 Epalinges, Switzerland
[2]Centro Internacional de Entrenamiento e Investigaciones Médicas, CIDEIM, Cali 760031, Colombia
[3]Universidad Icesi, Cali 760031, Colombia
[4]Lausanne Genomic Technologies Facility, University of Lausanne, 1015 Lausanne, Switzerland
[5]Lead contact
*Correspondence: miriam.diazvarela@unil.ch (M.D.-V.), fabienne.tacchini-cottier@unil.ch (F.T.-C.)
https://doi.org/10.1016/j.isci.2024.109773

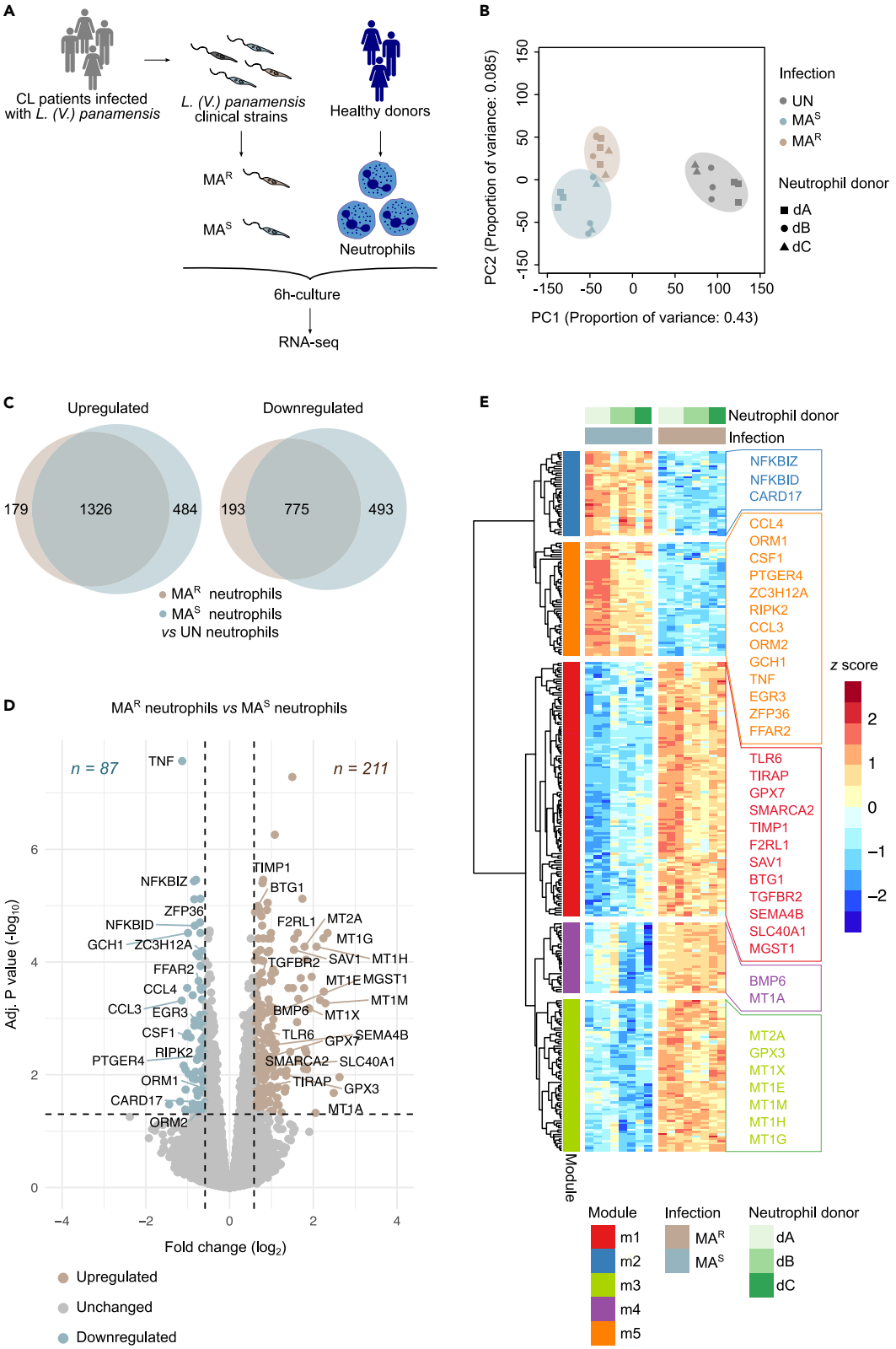
A
CL patients infected with L. (V.) panamensis
L. (V.) panamensis clinical strains
Healthy donors
MA^R
MA^S
Neutrophils
6h-culture
RNA-seq
B
PC2 (Proportion of variance: 0.085)
PC1 (Proportion of variance: 0.43)
Infection
UN
MA^S
MA^R
Neutrophil donor
dA
dB
dC
C
Upregulated
Downregulated
179
1326
484
193
775
493
MA^R neutrophils
MA^S neutrophils
vs UN neutrophils
D
MA^R neutrophils vs MA^S neutrophils
n = 87
n = 211
Adj. P value (-log10)
Fold change (log2)
Upregulated
Unchanged
Downregulated
E
Neutrophil donor
Infection
z score
Module
Infection
Neutrophil donor
m1
m2
m3
m4
m5
MA^R
MA^S
dA
dB
dC

Figure 1. Natural *Leishmania* antimony resistance regulates neutrophil gene expression program

(A) Schematic description of the transcriptomics approach.

(B) PCA plot of individual samples from UN, MA^S-, and MA^R-infected neutrophils from three donors. Proportion of variance is shown on axes.

(C) Intersection between genes upregulated or downregulated in MA^S vs. UN neutrophils and MA^R vs. UN neutrophils (cut-off: adjusted (adj.) $p < 0.05$; log_2Fold Change (FC) > 2 or < -2).

(D) Volcano plot depicting DEGs between MA^R vs. MA^S neutrophils (cutoff: adj. $p < 0.05$; $log_2FC > 1.5$ or < -1.5). The x and y axes indicate the expression FC (log_2) and adj. p value (-log_{10}) for each gene, respectively.

(E) Heatmap displaying normalized expression level (Z score) of DEGs between MA^R vs. MA^S neutrophils. The dendrogram represents hierarchical clustering of gene modules defined using correlation distance. See also Figure S1, Tables S1 and S2.

neutrophils are differentially activated upon infection with parasites of distinct susceptibility to antileishmanial drugs.[17,18] However, the interplay between DR and neutrophils and how these interactions might shape the outcome of infection is still unclear.

To gain further understanding of the role of neutrophils in infections with naturally drug-resistant *Leishmania* parasites, we have profiled the gene expression of human neutrophils in response to clinical *L. (V.) panamensis* strains causing cutaneous leishmaniasis (CL) that show distinct natural susceptibility to antimony. This analysis revealed that parasites having natural antimony resistance significantly modulate the neutrophil transcriptional profile, reducing cytokine expression among other changes. We further validated the impact of naturally drug-resistant parasites on neutrophil cytokine production at the protein level and showed that cytokine secretion by neutrophils regulates myeloid cell recruitment. Furthermore, using a murine model of CL, we confirmed that infection with naturally drug-resistant parasites influences the early myeloid cell recruitment at the site of infection.

RESULTS

Neutrophils infected with *Leishmania* of distinct natural antimony susceptibility show different gene expression profiles

To determine the involvement of neutrophils during infection with naturally drug-resistant *Leishmania* parasites, we conducted RNA sequencing (RNA-Seq) to evaluate the gene expression profiles of neutrophils isolated from peripheral blood of healthy donors infected with strains of distinct natural susceptibility to MA (Figure 1A). Human neutrophils were isolated with a multistep approach that combined blood density centrifugation and immunomagnetic negative selection of polymorphonuclear leukocytes that gave 99% neutrophil purity (Figure S1A). The parasite strains were isolated from lesions of CL patients, identified as *L. (V.) panamensis* by monoclonal antibodies[19] and isoenzyme electrophoresis,[20] and their susceptibility to MA was evaluated *in vitro* as previously described.[21] Importantly, these clinical strains were cryopreserved after isolation and propagated over a maximum of four passages during experimental analyses in order to limit change in the characteristics that they presented during infection in the patients. The characteristics of *L. (V.) panamensis* clinical strains with distinct susceptibility and their corresponding symbols are shown in Table S1. Gene expression profiles of infected neutrophils were compared with that of uninfected (UN) neutrophils. Principal-component analysis (PCA) of the expression of neutrophil genes in response to infection with parasites that were susceptible (MA^S) or resistant (MA^R) to MA, and uninfected, revealed that the largest sources of variance were the infection status and donor variability (Figure S1B). PCA of donor-adjusted data showed that the principal component 1 (PC1) separated uninfected and infected neutrophils, whereas PC2 discriminated neutrophils infected with MA^S and MA^R, indicating that a large portion of the transcriptional variation among samples was driven by the parasite susceptibility to MA (Figure 1B).

Differential expression analysis of infected and uninfected neutrophil samples identified more differentially expressed genes (DEGs) in neutrophils infected with drug-susceptible parasites than in those infected with drug-resistant parasites. Neutrophils exposed to MA^R parasites upregulated fewer unique genes (179) than those infected with MA^S parasites (484). Similarly, fewer unique genes were downregulated in neutrophils upon infection with MA^R parasites (193) compared with the number of unique downregulated genes in neutrophils infected with MA^S parasites (493) (Figures 1C and S1C; Table S2). To identify more accurately genes whose expression is regulated during infection with naturally MA^S or MA^R parasites in human neutrophils, we conducted a differential expression analysis between neutrophils exposed to MA^R parasites or MA^S parasites. This analysis led to the identification of 211 genes upregulated in neutrophils infected with drug-resistant parasites and 87 genes that were upregulated in neutrophils infected with drug-susceptible parasites (Figure 1D; Table S2). We next used clustering analysis to identify gene patterns associated with neutrophil exposure to MA^R or MA^S parasites. Two gene modules were overexpressed in transcriptomes of neutrophils exposed to susceptible parasites (modules 2 and 5), and three gene modules were upregulated in neutrophils infected with resistant parasites (modules 1, 3, and 4) (Figure 1E). Collectively, these data indicate that the neutrophil gene expression program induced by naturally antimony-resistant parasites significantly differs from the one induced by susceptible strains.

Parasites having natural antimony resistance trigger detoxification and limit pro-inflammatory transcriptional circuits in neutrophils

To identify potential mechanisms associated with the neutrophil-DR parasite interplay, we examined the underlying biological processes involved in the transcriptional changes in neutrophils infected with parasites of divergent susceptibility phenotype to MA (MA^R vs. MA^S) using gene set enrichment analysis (GSEA). GSEA of the neutrophil DEGs against the hallmark gene sets of the Molecular Signatures Database (MSigDB)[22,23] revealed 14 significantly enriched signatures. Naturally drug-susceptible parasites induced an increased expression of neutrophil genes that were mainly associated with signatures involved in inflammation ("inflammatory response," "allograft rejection") and immune activation status ("tumor necrosis factor alpha [TNF-α] signaling via NF-κB," "interleukin-6 [IL-6] JAK STAT3 signaling," "interferon α

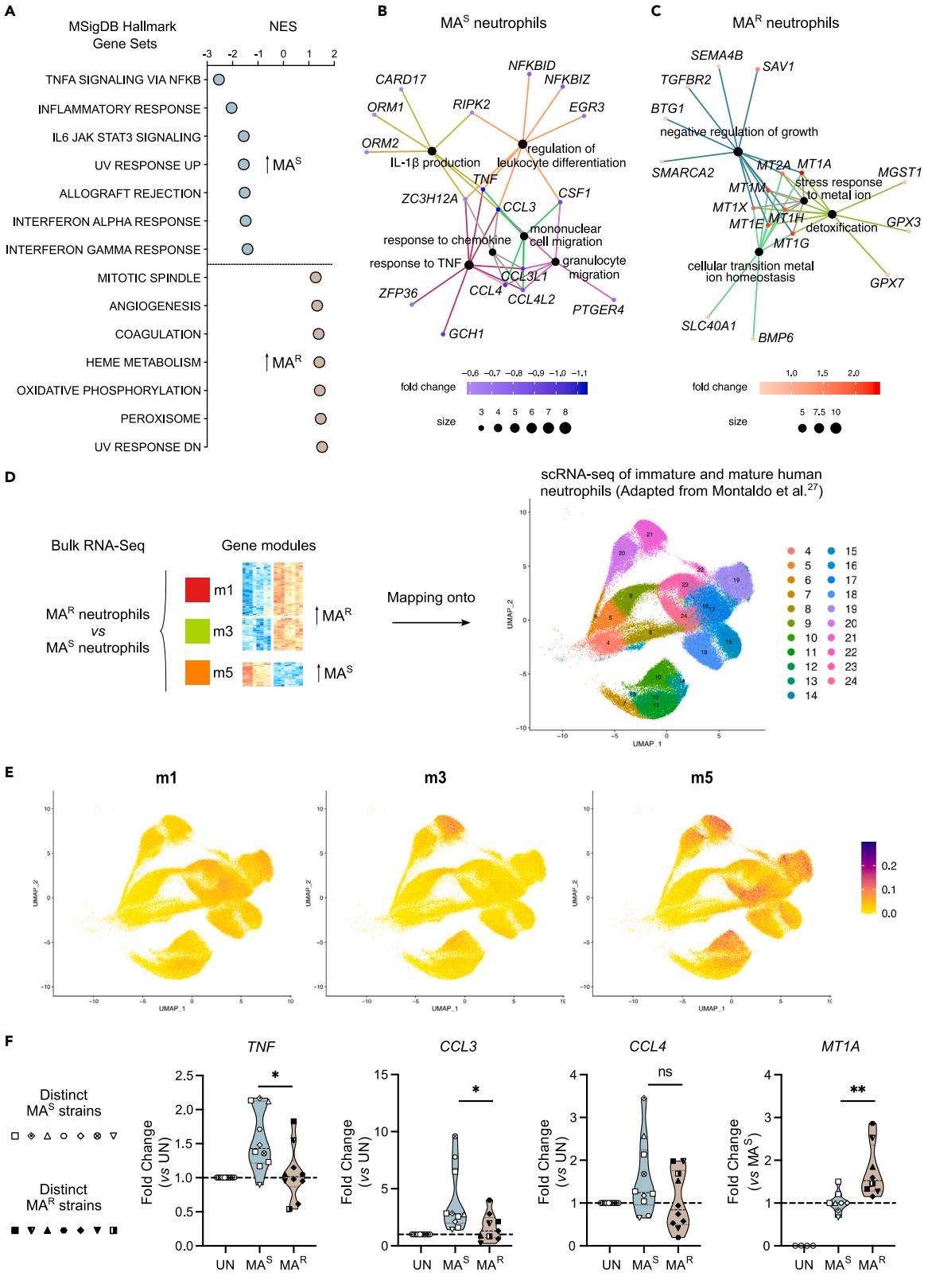
A
MSigDB Hallmark Gene Sets
NES
TNFA SIGNALING VIA NFKB
INFLAMMATORY RESPONSE
IL6 JAK STAT3 SIGNALING
UV RESPONSE UP
ALLOGRAFT REJECTION
INTERFERON ALPHA RESPONSE
INTERFERON GAMMA RESPONSE
MITOTIC SPINDLE
ANGIOGENESIS
COAGULATION
HEME METABOLISM
OXIDATIVE PHOSPHORYLATION
PEROXISOME
UV RESPONSE DN
↑MA^S
↑MA^R
B
MA^S neutrophils
NFKBID
NFKBIZ
CARD17
ORM1
RIPK2
EGR3
ORM2
regulation of leukocyte differentiation
IL-1β production
TNF
ZC3H12A
CCL3
CSF1
mononuclear cell migration
response to chemokine
response to TNF
granulocyte migration
CCL3L1
CCL4
CCL4L2
ZFP36
PTGER4
GCH1
fold change
size
C
MA^R neutrophils
SEMA4B
SAV1
TGFBR2
BTG1
negative regulation of growth
SMARCA2
MT2A
MT1A
MGST1
stress response to metal ion
MT1M
MT1X
MT1E
MT1H
detoxification
GPX3
MT1G
cellular transition metal ion homeostasis
GPX7
SLC40A1
BMP6
fold change
size
D
Bulk RNA-Seq
Gene modules
MA^R neutrophils
vs
MA^S neutrophils
m1
m3
m5
↑MA^R
↑MA^S
Mapping onto
scRNA-seq of immature and mature human neutrophils (Adapted from Montaldo et al.[27])
UMAP_1
UMAP_2
E
m1
m3
m5
F
Distinct MA^S strains
Distinct MA^R strains
TNF
CCL3
CCL4
MT1A
Fold Change (vs UN)
Fold Change (vs MA^S)
UN
MA^S
MA^R
*
**
ns

Figure 2. Transcriptional signatures of neutrophils infected with antimony-resistant parasites are associated with detoxification and limited immune activation

(A) Gene set enrichment analysis (GSEA) of DEGs identified between MA^R vs. MA^S neutrophils against hallmark gene sets of the Molecular Signatures Database (MSigDB). Signatures significantly enriched (cutoff: adj. $p < 0.05$) in downregulated and upregulated genes are marked in blue and brown, respectively. x axis represents the normalized enrichment score (NES) for each hallmark signature.

(B and C) Gene ontology (GO) and network analysis of DEGs between MA^R vs. MA^S neutrophils, (B) overexpressed in MA^S neutrophils or (C) MA^R neutrophils. Fold change of expression of downregulated or upregulated genes is marked in blue or red, respectively. The size of each GO term represents the number of DEGs associated with each term.

(D and E) Mapping of the main gene modules identified between MA^R vs. MA^S neutrophils (see Figure 1E) onto scRNA-Seq data of mature and immature human neutrophils (clusters 4–24) described by Montaldo et al.[26] (D) Schematic description of the mapping approach and (E) UMAP plots showing the expression of the gene modules.

(F) Expression analyzed by RT-qPCR of selected DEGs in neutrophils exposed to the indicated distinct MA^S and MA^R strains. Fold change was calculated as described in the STAR Methods. Each dot represents one neutrophil donor, and each symbol indicates one *L. (V.) panamensis* strain. Results are combined from four independent experiments. $*p < 0.05$, $**p < 0.01$, as calculated by Mann Whitney U test. ns, non-significant. See also Figures 1 and S2, Tables S1 and S2.

response," and "interferon γ response"). On the other hand, drug-resistant parasites induced the upregulation of genes related to metabolism and detoxification ("peroxisome," "oxidative phosphorylation," "heme metabolism") (Figure 2A). We then subjected the set of genes upregulated in neutrophils after infection with susceptible or resistant parasites to Gene Ontology (GO) enrichment analysis. The neutrophil response to susceptible parasites was characterized by the expression of genes involved in pro-inflammatory responses, denoted by the enrichment in categories such as "interleukin-1β production" (*TNF, CARD17, ORM1, ORM2*) as well as "response to chemokine" and "cell migration" (*CCL3, CCL4*) (Figure 2B). Natural antimony-resistant parasites upregulated the expression of genes associated with GO categories of "detoxification" and "stress response to metal ions" among others (Figure 2C). These categories were mainly interconnected by genes encoding metallothioneins (*MT1A, MT2A, MT1X, MT1E, MT1H, MT1G*), small metal-binding proteins involved in the homeostatic regulation of heavy metals, and protection against oxidative stress.[24,25]

Neutrophil heterogeneity has been reported, including in inflammatory conditions, with distinct immunomodulatory functions.[27] To provide further insights into the impact of parasite antimony resistance on the neutrophil transcriptome and neutrophil heterogeneity, we mapped the gene modules obtained in our bulk transcriptomic profiling onto the single-cell RNA-Seq (scRNA-Seq) analysis of human neutrophils at steady state and upon stress recently reported by Montaldo et al.[26] In that study, a high diversity of neutrophils was observed based on their transcriptome profile, which reflected their maturation stage, tissue location, exposure to stress signals, and donor/patient identity. Given the peripheral blood origin of the neutrophils analyzed in this present study, we mapped the main three neutrophil gene modules impacted by antimony susceptibility (Figure 1E) onto the scRNA-Seq data from mature and immature neutrophil populations (clusters 4–24)[26] (Figure 2D), which were visualized by uniform manifold approximation project (UMAP) embedding (Figure 2E). Remarkably, specific neutrophil clusters defined in the study of Montaldo et al.[26] preferentially transcribed some of DEGs identified in our bulk RNA-Seq analysis (Figures 2E and S2). In line with the peripheral blood origin of our samples, most of the genes were expressed by mature populations (15–24). Module 1 (m1) had the most ubiquitous expression among the clusters, which were characterized by a higher expression of transcripts involved in control of gene expression (*CEBPD, MIDN*) as well as cell growth and differentiation (*BTG1*) (Figure S2A). In contrast, the expression of modules 3 (m3) and 5 (m5) was more restricted to specific clusters. Notably, certain genes from m3, such as those encoding for metallothioneins *MT1X* and *MT2A*, were preferentially expressed by clusters 9, 10, 20, and 21 (Figure S2B). Additionally, clusters 20 and 21 also had significant expression of *SOCS3*, a suppressor of cytokine signaling. Neutrophil populations expressing m5 genes, which were downregulated upon infection with MA^R parasites, were characterized by a high expression of genes involved in the regulation of inflammation (*ORM1, ZEB2, ZFP36, FFAR2, PLEK*), mainly associated with clusters of mature neutrophils, except for *ORM1* and *ZEB2*, which exhibited an increased expression in clusters 6 and 10, respectively (Figure S2C). Collectively, these results show that specific neutrophil subsets could be associated with the neutrophil response to antimony-resistant parasites.

To validate our RNA-Seq findings in a larger sample of *Leishmania* strains of distinct natural antimony susceptibility and with an increased number of neutrophil donors, we conducted qPCR expression analyses of selected neutrophil genes that were most differentially expressed and highlighted by gene enrichment analyses. These analyses revealed similar neutrophil expression patterns to those evidenced by RNA-Seq, which were characterized by, among other transcriptional changes, a decrease in the expression of cytokine-encoding genes and an increase of metallothionein-coding genes in neutrophils infected with resistant parasites compared with those exposed to susceptible parasites (Figure 2F). Using neutrophils isolated from multiple donors, we have thus extended and validated our neutrophil transcriptomics data to other naturally MA^R and MA^S *L. (V.) panamensis* strains.

Neutrophil infection by natural antimony-resistant parasites reduces cytokine production and migration of myeloid cells

Our neutrophil gene expression profiling showed that parasite antimony resistance modulated the expression of multiple genes coding for cytokines and chemokines. We thus sought to investigate whether these transcriptional changes led to differential expression at the protein level with potential functional consequences. We selected a panel of thirteen secreted proteins that included cytokines, chemokines, growth factors, and other signaling molecules encoded by DEGs identified in the DEA between neutrophils infected with parasites of divergent susceptibility phenotypes to antimony (MA^R vs. MA^S) (Figure S3A) or between infected and uninfected neutrophils (MA^R vs. uninfected; MA^S vs.

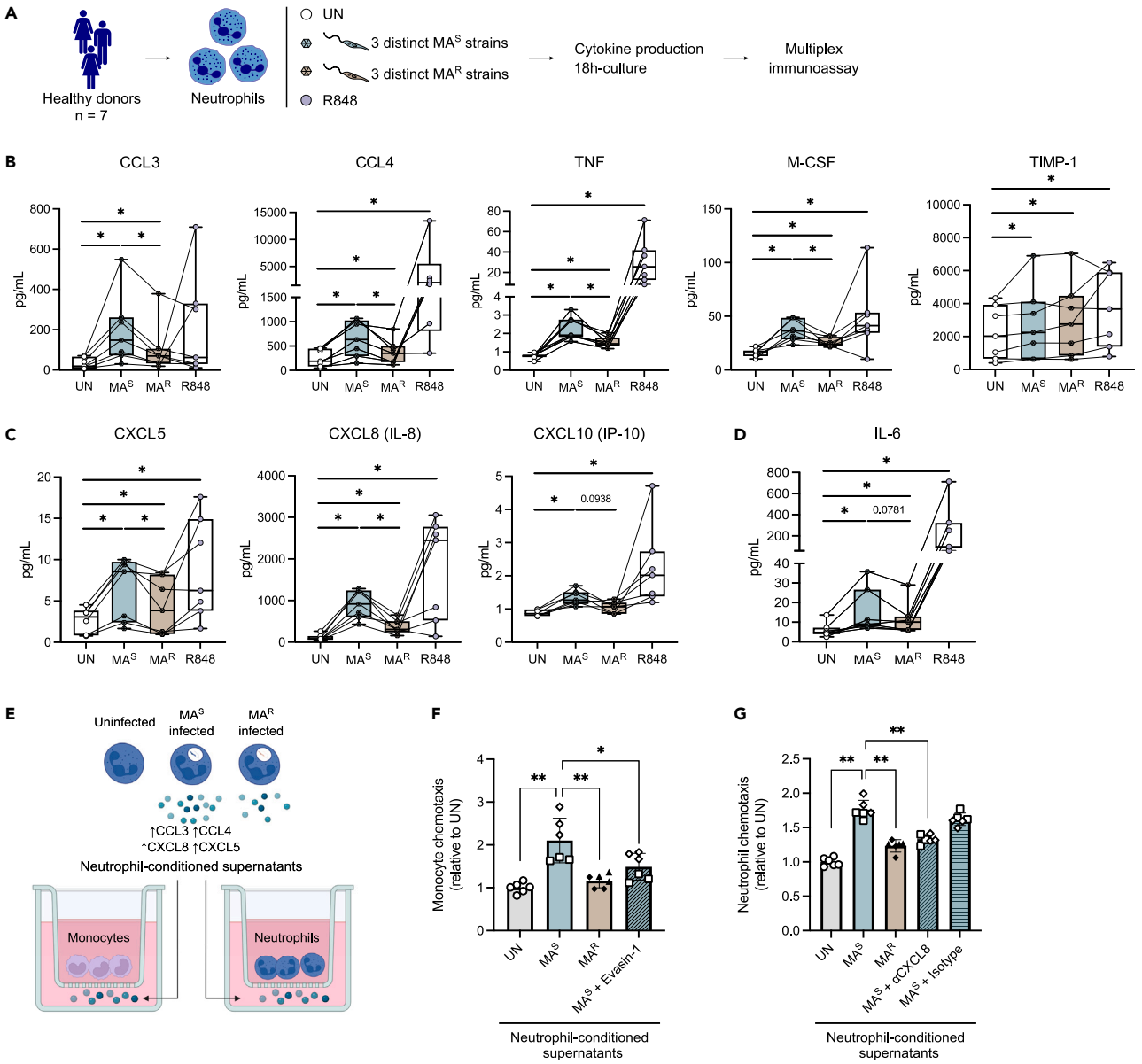

Figure 3. Cytokine release and chemoattractant capacity of neutrophils are impaired upon infection with antimony-resistant *Leishmania* parasites

(A) Experimental design of the multiplex immunoassay.

(B–D) Cytokine/chemokine levels in the indicated neutrophil-conditioned supernatants derived from unstimulated, MA^R- or MA^S-infected or R848-activated neutrophils of (B) cytokines encoded by DEGs between MA^R vs. MA^S neutrophils, (C) CXC chemokines, and (D) IL-6. Lines connect values obtained per neutrophil donor among the conditions assessed. Mean values from three distinct parasite strains assessed per neutrophil donor are presented in the infected conditions (⊛). Min, max, median, and 25%–75% interquartile range are presented.

(E) Schematic description of transwell assays.

(F) Chemotaxis of monocytes toward indicated neutrophil supernatants that were pre-incubated or not with Evasin-1 for CCL3 neutralization.

(G) Chemotaxis of neutrophils toward neutrophil supernatants that were pre-incubated or not with CXCL8-neutralizing or isotype-matched antibodies. In the chemotaxis assays, pooled data from two independent experiments is shown. The indicated symbol represents the infecting parasite strain used to obtain neutrophil-conditioned supernatants or uninfected neutrophils (○). Bar plots present mean with SD values. *$p < 0.05$, **$p < 0.01$, ***$p < 0.001$, as calculated by Wilcoxon test (B–D) or Mann Whitney U test (F and G). UN, uninfected. ns, non-significant. See also Figure S3 and Table S1.

uninfected) (Figure S3B). Using multiplex immunoassay, we measured the levels of these soluble proteins in the culture supernatants of neutrophils isolated from different donors and cocultured with parasite strains of different antimony susceptibility for 18 h. The mean value per donor measured in supernatants of neutrophils infected with each of the three strains separately is shown (Figure 3A). As controls, we

quantified the protein release from uninfected neutrophils (UN) that were treated or not with resiquimod (R848), a TLR7/8-agonist known to trigger cytokine production in human neutrophils.[28] We observed distinct protein release between neutrophils infected with parasites of disparate susceptibility profile to antimony, correlating with most of the transcriptional changes evidenced in the DEA of the analyzed cytokines (Figures 3B and S3A). Infection with MA^S parasites induced CCL3 and CCL4 release by neutrophils, whereas the induction was markedly reduced in MA^R-infected neutrophils. Neutrophils infected with MA^S strains produced low levels of TNF and macrophage colony-stimulating factor (M-CSF) that were all also significantly reduced in neutrophils infected with MA^R strains. The TIMP metallopeptidase inhibitor 1 (TIMP1) was not differentially released by neutrophils infected with strains of varying antimony susceptibility (Figure 3B), unlike the other genes that followed the transcriptomics differential gene expression observed (Figure S3A).

The correspondence between gene expression and released protein was more limited in the genes identified in the DEA between infected and uninfected neutrophils (Figures 3C, 3D, and S3B). We observed increased CXCL5 and CXCL8 chemokine secretion following *Leishmania* infection, in agreement with our transcriptional analyses. Importantly, the neutrophil-attracting chemokines CXCL5 and CXCL8 were released at higher levels by neutrophils upon infection with MA^S parasites compared with those infected with MA^R parasites (Figure 3C), a profile that was not observed by RNA-Seq (Figure S3B). We observed low levels of the interferon-gamma-induced protein 10 (IP-10, CXCL10) released by neutrophils infected with MA^S parasites, which were decreased in neutrophils infected with MA^R parasites, in line with the transcriptional data (Figures 3C and S3B). In addition, neutrophils infected with MA^S parasites had an increased tendency to secrete IL-6 (Figure 3D), a pro-inflammatory cytokine whose expression was specifically upregulated upon infection with susceptible strains (Figure S3B). On the other hand, we did not observe any differences in the release of Fas, VEGF-R1, CD48, and SCGF beta under the conditions evaluated (Figure S3C), despite some changes in gene expression that had been evidenced by transcriptomic analysis (Figure S3B).

We next determined the biological impact of parasite antimonial susceptibility on the differential cytokine secretion by neutrophils. The release of several chemokines was suppressed in neutrophils infected with antimony-resistant parasites; we thus hypothesized that neutrophil-mediated recruitment of immune cells could be affected in infections with naturally drug-resistant parasites. In particular, the differential neutrophil production of CCL3 and CXCL8 could significantly alter the recruitment of monocytes and neutrophils, respectively. To address this question, we tested the capacity of supernatants from neutrophils infected with MA^S or MA^R strains to chemoattract primary human monocytes and neutrophils using transwell cell migration assays (Figure 3E). Monocyte chemotaxis assays demonstrated that supernatants from neutrophils infected with MA^S parasites had an increased chemoattractant activity for monocytes compared with supernatants derived from neutrophils infected with resistant parasites or uninfected (UN) neutrophils (Figure 3F). Moreover, this activity was dependent on CCL3 because monocyte migration was significantly suppressed in supernatants treated with Evasin-1, a highly selective neutralizing protein shown to bind CCL3 with high affinity and CCL4 with lower affinity[29] (Figures 3F and S3D). Similarly, increased neutrophil migration was observed toward supernatants derived from neutrophils infected with MA^S parasites, but not toward supernatants derived from neutrophils infected with MA^R strains. CXCL8 was found to act as a key chemokine in this context because neutrophil recruitment was significantly decreased by pre-treatment of supernatants with CXCL8-neutralizing, but not isotype-matched, antibodies (Figure 3G). Collectively, our data highlight the relevance of the influence of parasite antimony resistance in neutrophil cytokine production and suggest a novel role of neutrophils in the modulation of host immune cell recruitment during drug-resistant *Leishmania* infections.

TLR8 signaling contributes to the distinct neutrophil cytokine release upon infection with naturally drug-susceptible or -resistant parasites

We show that similar cytokines are induced in neutrophils infected with MA^S parasites or stimulated with resiquimod (R848), the TLR7/8-agonist, even though, resiquimod induced higher levels of secretion. In contrast, neutrophils infected with MA^R parasites released generally low cytokine levels. We further investigated possible similarities between MA^S- and TLR8-stimulated human neutrophils at the transcriptomic level. To this end, we compared the genes differentially expressed in transcriptome of neutrophils infected with MA^R vs. MA^S parasites with that of genes induced in R848-activated neutrophils[28] (Figures S4A and S4B). The gene set enrichment analysis (GSEA) revealed that genes upregulated upon infection with MA^S parasites resembled those upregulated with R848 (clusters 3, 8, and 9) (Figure 4A), which include *ORM1*, *TNF*, and *CCL3* (Figure S4B). In contrast, genes overexpressed in neutrophils upon infection with MA^R parasites are enriched in genes downregulated in response to R848 (Cluster 2) (Figure 4A), including *RUNX2*, *F2RL1*, and *SLC40A1* (Figure S4B). These findings suggest that infection with MA^S parasites triggers similar pathways than TLR8 signaling, whereas infection with MA^R parasites does not. To further investigate the importance of TLR8 signaling in the difference observed in cytokine release by neutrophils infected with naturally MA^S or MA^R parasites, we blocked TLR8 signaling with CU-CPT9a, a specific TLR8 antagonist. Blocking was efficient as shown by the loss of CCL3 and CXCL8 secretion in R848-treated neutrophils in presence of the inhibitor (Figure 4B), in line with previous report.[30] We then infected neutrophils with MA^S or MA^R parasites, in presence or absence of the TLR8 inhibitor. Blocking of TLR8 prevented CCL3 and markedly decreased CXCL8 secretion by MA^S-infected neutrophils, whereas minor impact was observed in MA^R-infected neutrophils (Figure 4C). Collectively, these results suggest that natural resistance to antimony contributes to an altered human neutrophil response characterized by limited immune activation, in which dampening of TLR8 signaling plays a role.

Natural antimony-resistant parasites impair early myeloid recruitment at the site of infection

To verify whether parasite antimony resistance might influence myeloid recruitment at the site of *L. (V.) panamensis* infection, we used a BALB/c mouse model that reproduces the immune response in human CL infection caused by this *Leishmania* species.[31] Neutrophils are among the first cells recruited to the site of infection, and their rapid cytokine release modulates the recruitment of other cells[32–36]; we thus first assessed

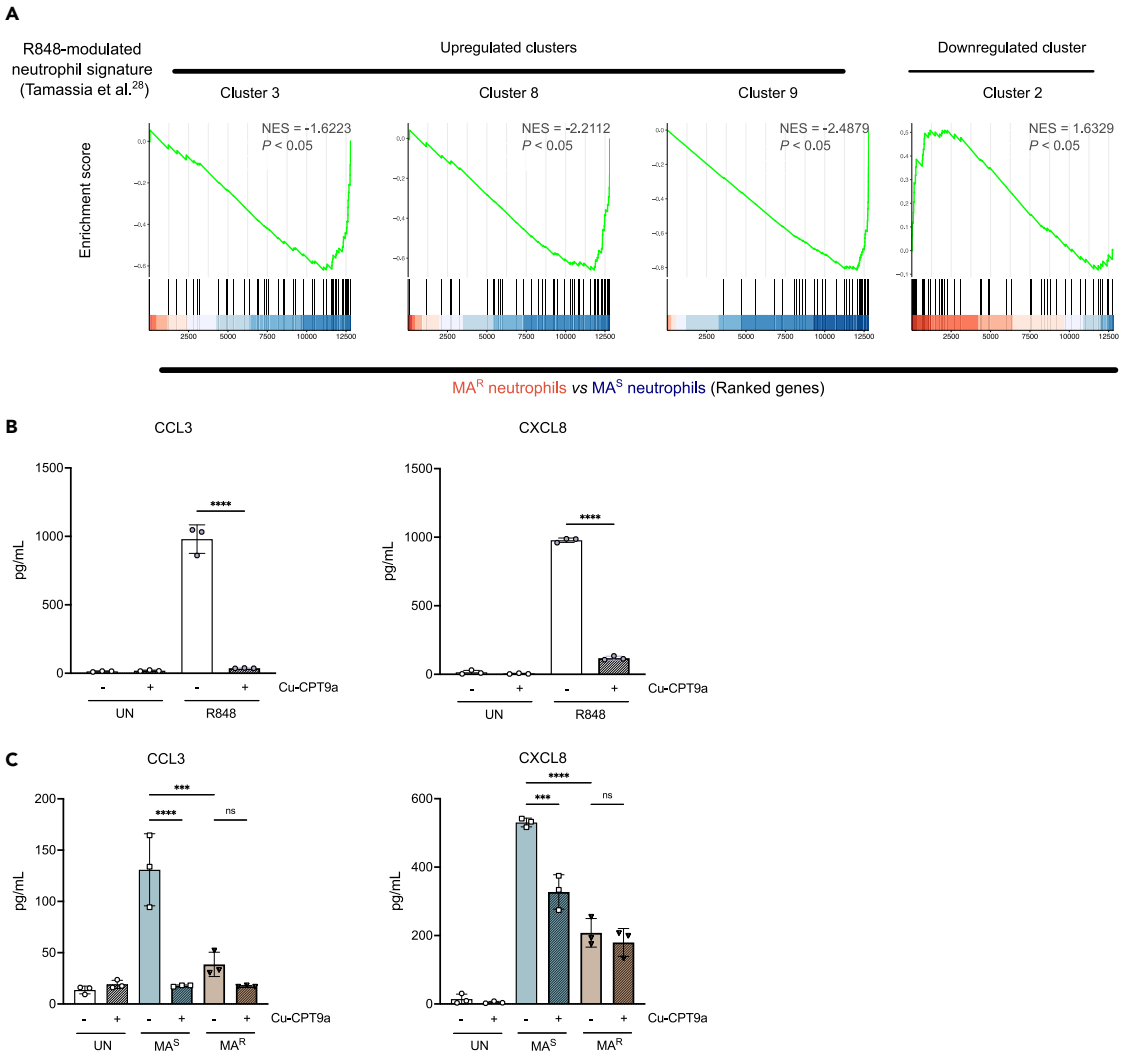

Figure 4. TLR8 signaling contributes to the distinct neutrophil cytokine release upon infection with naturally drug-susceptible or -resistant parasites

(A) GSEA plots depict gene signatures associated with neutrophils upon TLR8 activation with R848, as described in the study of Tamassia et al.[28] tested against the ranked gene list for MA^R vs. MA^S neutrophils reported in our study. The Running Enrichment Score (depicted by the green line) represents the analysis as it progresses through the ranked gene list. The black lines on the Enrichment Score plot indicate the positions of gene set members within the ranked list of genes. NES, normalized enrichment score.

(B) Cytokine release by uninfected ± R848-treated neutrophils in the presence or absence of the TLR8-specific antagonist CU-CPT9a.

(C) CCL3 and CXCL8 release by neutrophils infected with naturally MA^R or MA^S parasites in the presence or absence of CU-CPT9a. Data shown are representative of three independent experiments. Bar graphs present mean with SD values. ***$p < 0.001$, ****$p < 0.0001$, as calculated by two-way ANOVA. UN, unstimulated. ns, non-significant.

See also Figure S4 and Table S1.

whether murine bone marrow neutrophils (BMNs) isolated from BALB/c mice respond to clinical *Leishmania* strains having distinct antimony susceptibility in a similar way as human neutrophils. We observed an increased ROS production in murine BMNs exposed to MA^S parasites compared with those infected with MA^R strains (Figure 5A), concurring with previous findings reported in human neutrophils.[18] Neutrophils were exposed to phorbol myristate acetate (PMA), a well-known inducer of ROS as a positive control, and to diphenyleneiodonium chloride (DPI), an inhibitor of ROS, as a negative control. In addition, we assessed by ELISA the release of TNF and CCL3, two of the most differentially secreted cytokines observed after infection of human neutrophils with MA^R and MA^S parasites. Similarly to human blood neutrophils, murine BMNs infected with antimony-resistant strains showed lower TNF and CCL3 production (Figure 5B). CXCL1 (KC) and CXCL2 (MIP-2) are the murine homologues of human CXCL8. In response to MA^S infection, no detectable CXCL1 release was observed in infected neutrophils. However, CXCL2 was selectively produced by neutrophils infected with MA^S strains, as observed for CXCL8 in human neutrophils, but to lower levels (Figure 5C).

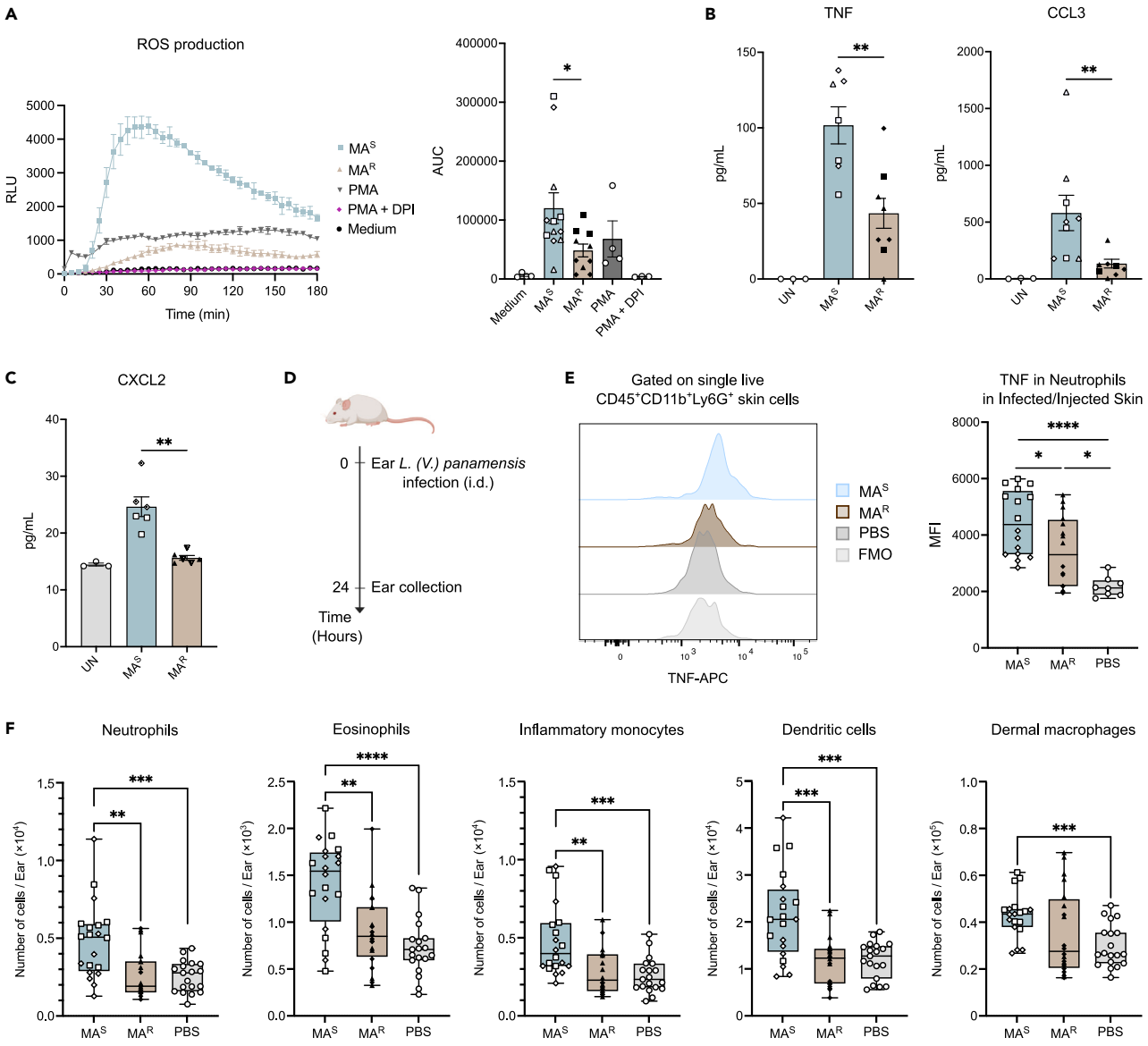

Figure 5. Antimony-resistant *Leishmania* parasites induce similar responses in murine and human neutrophils and limit early myeloid cell recruitment in a murine model of CL

(A) Representative curves of chemiluminescent signal and the corresponding area under the curve (AUC) of ROS produced by murine BMNs exposed to the indicated conditions.

(B and C) Cytokine concentration in supernatants of murine BMNs exposed or not to parasites for 18 h of (B) murine TNF and CCL3 and (C) CXCL2.

(A–C) Bar graphs present the mean of biological replicates with SD values.

(D) Infection with MA^S or MA^R *L. (V.) panamensis* parasites, or injection with PBS, was performed i.d. on BALB/c mice. After 24 h ear skin tissue was harvested and processed for flow cytometry analysis.

(E) Representative flow cytometry plot for the indicated experimental conditions (left panel) and median fluorescence intensity (MFI) of TNF expression in neutrophils in the infected/injected skin.

(F) Total number of neutrophils, eosinophils, inflammatory monocytes, dendritic cells, and dermal macrophages per infected/injected ear.

(E and F) Plots present min, max, median, and 25%–75% interquartile range. Each dot represents one ear, and each symbol indicates one *L. (V.) panamensis* strain. Results are combined from two independent experiments. *$p < 0.05$, **$p < 0.01$, ***$p < 0.001$, ****$p < 0.0001$, as calculated by Mann Whitney U test. See also Figure S5 and Table S1.

To validate these results *in vivo*, BALB/c mice were infected intradermally in the ear with MA^R or MA^S *L. (V.) panamensis* strains or injected with a similar volume of PBS (Figure 5D). Twenty-four hours post-infection, ear tissue was recovered, and cells were isolated and stained to perform flow cytometry analysis of intracellular TNF in neutrophils (Figures 5E and S5A). In line with our *in vitro* findings, TNF expression in

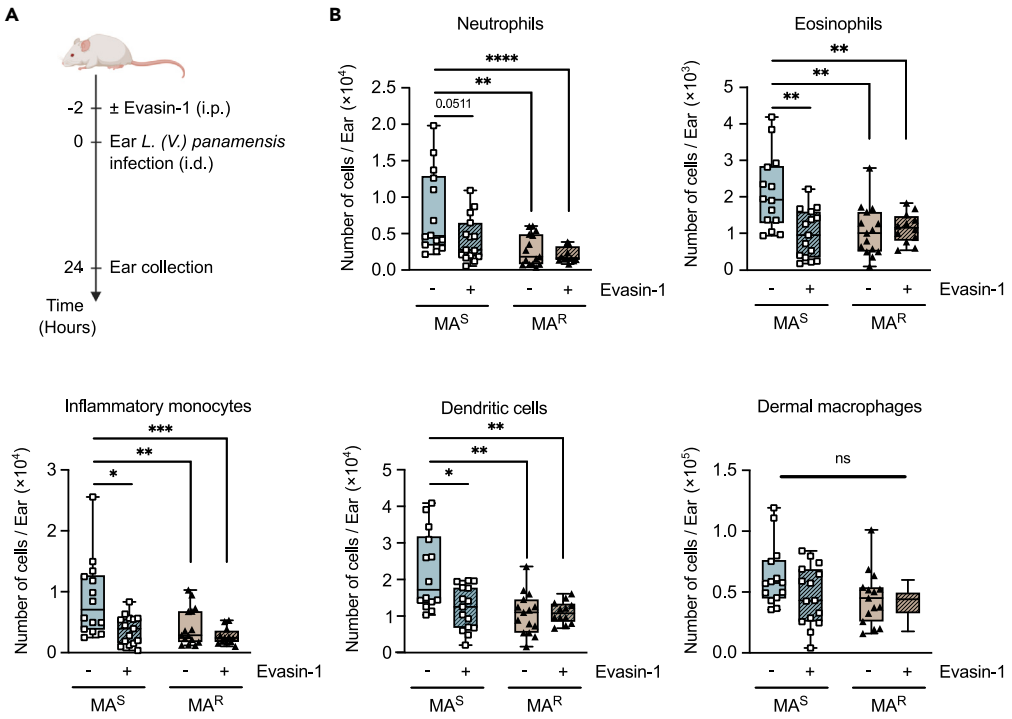

Figure 6. Antimony-resistant *Leishmania* parasites impair CCL3-driven early myeloid cell recruitment at the site of infection

(A) Experimental *in vivo* approach for CCL3 blockade. BALB/c mice were injected with Evasin-1, a chemokine binding protein that neutralizes CCL3, or PBS as a control, prior to i.d. parasite infection. Twenty-four hours post-infection, the infected tissue was harvested and cells were isolated and stained for flow cytometry analysis.

(B) Total number of neutrophils, eosinophils, inflammatory monocytes, dendritic cells, and dermal macrophages per infected ear. Plots present min, max, median, and 25%–75% interquartile range. Each dot represents one ear and each symbol indicates an *L. (V.) panamensis* strain. Results are combined from two independent experiments. *$p < 0.05$, **$p < 0.01$, ***$p < 0.001$, ****$p < 0.0001$, as calculated by Mann Whitney U test. ns, non-significant.

See also Figure S5 and Table S1.

neutrophils was significantly increased in infected skin of mice infected with MA^S parasites compared with those challenged with MA^R parasites as shown by median fluorescence intensity (Figure 5E), TNF^+ neutrophil frequency (12 ± 1.6 vs. 6.5 ± 0.7%) and number (514 ± 118 vs. 192 ± 40) in MA^S- vs. MA^R-infected neutrophils, respectively. Overall, these results show that the responses of murine neutrophils toward clinical strains having natural disparate antimony susceptibility mirror those observed in human neutrophils. We next assessed whether the antimony-dependent modulation of myeloid cell recruitment observed in human neutrophils *in vitro* was also taking place *in vivo*. To this end, we infected intradermally BALB/c mice with *L. (V.) panamensis* strains of distinct antimony susceptibility and quantified $CD45^+CD11b^+Ly6G^+$ neutrophils, $CD45^+CD11b^+SiglecF^+$ eosinophils, $CD45^+CD11b^+Ly6C^{high}$ inflammatory monocytes, $CD45^+CD11c^+$ dendritic cells (DCs), and $CD45^+CD11b^+CD206^{high}$ dermal macrophages in the skin 24 h post-infection using flow cytometry analysis (Figure S5B). A significantly higher number of neutrophils, eosinophils, monocytes, and DCs was observed in mice infected with naturally drug-susceptible parasites compared with those infected with drug-resistant parasites or PBS-injected control, except for dermal macrophages, for which no differences were found between responses to susceptible and resistant strains (Figure 5F). These results demonstrate that antimony-resistant parasites dampen host myeloid responses at the early stage of infection.

In vivo immune recruitment in the context of antimony susceptibility is dependent on CCL3

We show here that CCL3 secretion by neutrophils is poorly induced following infection with antimony-resistant *L. (V.) panamensis* parasites. Neutrophil-derived CCL3 was previously shown to be essential in the recruitment of DCs early in *L. major* infection.[37] To further assess the role of CCL3 in infections with *L. (V.) panamensis* having distinct antimony susceptibility, we transiently depleted CCL3 by treating mice with Evasin-1 (Figure 6A). Two hours before intradermal (i.d.) infection with MA^R or MA^S parasites, BALB/c mice were injected intraperitoneally with Evasin-1. Twenty-four hours post-infection, infected ear tissue was collected and processed for flow cytometry analysis of myeloid populations as previously described (Figure S5B). A small, though not statistically significant, decrease in the number of recruited neutrophils was observed in MA^S-infected mice treated with Evasin-1, and the number of recruited eosinophils, inflammatory monocytes, and DCs was significantly reduced at the site of infection in these mice compared with untreated mice infected with the MA^S strains (Figure 6B). In contrast, Evasin-1 treatment in mice infected with the MA^R strains did not result in any effect on the chemoattraction of the cell populations assessed,

in line with the low induction of CCL3 release by neutrophils and the poor chemoattractant activity that were observed in human neutrophils infected with MA^R parasites.

Overall, these findings demonstrate that the early innate response to antimony-resistant *L. (V.) panamensis* parasites at the infection site is characterized by a low TNF expression in neutrophils and a limited recruitment of myeloid cells. Early cellular recruitment is dependent on CCL3, one of the most differentially expressed genes in neutrophils exposed to parasites of divergent antimony susceptibility. These data underscore the role of neutrophils in the intersection between DR and immunity.

DISCUSSION

Antimicrobial DR and host immunity are critical factors mediating the clinical outcome of infectious diseases. Here, we investigated how the interactions between natural drug-resistant parasites and host immunity contribute to the outcome of infections. By evaluating the transcriptional response of primary human neutrophils exposed to clinical strains of *Leishmania* having natural resistance or susceptibility to MA, we provide compelling evidence that MA^R parasites induce a gene expression profile in neutrophils that differs from the one induced by MA^S parasites. The distinct transcriptional profile elicited by naturally drug-resistant parasites leads to an upregulation of detoxification circuits and a limited expression of genes related to immune activation. In addition, neutrophil infection with MA^R parasites results in reduced cytokine and chemokine transcription and release by neutrophils, which in turn reduced neutrophil ability to recruit myeloid cells. In this context, blocking of the chemokines CCL3 and CXCL8 in the supernatant of neutrophils infected with MA^S parasites confirmed their relevance in the recruitment of human monocytes and neutrophils, respectively. These results reveal that these chemokines could play an important role in antimony DR, suggesting that their reduced transcription and release could contribute to a less effective immune response upon infection with drug-resistant strains. Moreover, mice infected with drug-resistant strains showed a diminished early immune recruitment at the site of infection, confirming these data *in vivo*. This process was CCL3-dependent, a chemokine that was one of the most differentially expressed cytokines in both human and murine neutrophils upon infection with parasites of divergent antimony susceptibility. These findings support the relevance of CCL3 as a mediator of the immune response affected by parasite antimony resistance. Collectively, these findings revealed a novel role of neutrophils in the regulation of the host immune microenvironment during antimony-resistant *Leishmania* infections, thus discovering underlying mechanisms of natural DR related to neutrophil responses.

Neutrophil-derived chemokines are instrumental to instruct other immune cells as well as to recruit neutrophils themselves.[38] Here, we show that in the context of natural resistance to antimonial drug, parasites impaired the release of neutrophil chemokines and migration of innate immune cells. Interestingly, other studies have reported muted neutrophil responses upon infection with drug-resistant strains of bacteria such as *Staphylococcus aureus*.[39,40] Moreover, *L. infantum* parasites resistant to miltefosine, another widely used antileishmanial drug, have been shown to evade innate immune recognition in the presence of miltefosine, triggering limited activation of NK and NKT cells and enchancing parasite survival.[41] Of interest, antimony-resistant *L. donovani* parasites were shown to affect the *in vitro* response of macrophages,[42] DCs,[43] and regulatory T cells.[44] Differently from the clinical parasite strains that were evaluated in this work, these studies were performed using *Leishmania* parasites that induce a visceral form of the disease and that were cultured *in vitro* and maintained in golden hamsters following several passages. Here, we used clinical strains having distinct natural antimony susceptibility that were isolated from patients with cutaneous forms of the disease and minimally passaged *in vitro* in order to retain clinically relevant parasite populations. Notably, the different parasite strains analyzed in this study correspond to naturally occurring antimony-resistant and antimony-susceptible parasite populations that are characterized by specific isoenzyme profiles (zymodemes). Zymodemes were shown to correlate with resistance or susceptibility to antimony, but not to that of miltefosine, explicitly showing the specificity of natural antimony resistance in these populations of *L. (V.) panamensis*.[7] These findings underscore the value of the usage of naturally drug-resistant and drug-susceptible parasite populations to decipher the complex interactions between parasite DR, host cell responses, and treatment failure. Here, we show that neutrophils, the first cells arriving to the site of infection, differently orchestrate the recruitment of myeloid cells depending on the antimonial drug susceptibility status of the infecting *Leishmania* parasite. Therefore, evasion of immune responses could represent one potential strategy that has evolved in drug-resistant pathogen populations favoring their persistence, and neutrophils seem to play a crucial early role in this process.

Along this line, we observed a decreased early recruitment of myeloid cells at the site of infection in mice infected with MA^R parasites compared with mice infected with MA^S parasites. Neutralization of CCL3 with Evasin-1 reduced dramatically the recruitment of myeloid cells in mice infected with MA^S parasites. Notably, a protective role for the early release of neutrophil-derived CCL3 in experimental murine models of *Leishmania* infection and vaccination was previously reported.[37,45] This suggests that MA^R parasites might be dampening early protective neutrophil responses, which could potentially contribute to poor clinical outcomes in patients infected with drug-resistant parasites. In this line, BALB/c mice infected intradermally with MA^R *L. (V.) panamensis* clinical strains developed larger lesion size and had a higher parasite burden than mice infected with MA^S strains.[46] Interestingly, studies in CL patients infected with *L. (V.) panamensis* have associated treatment failure and chronicity of leishmaniasis with a sustained expression of monocyte- and neutrophil-associated chemokines.[47,48] Despite playing a deleterious role in sustained inflammation after treatment, chemokines, if released early after infection and/or before treatment, might still contribute to protective responses. Indeed, the study by Navas et al.[48] showed an increased expression of CCL2, the most potent monocyte chemoattractant, in the pretreatment lesion samples from cured patients compared with those coming from patients that failed treatment. Further investigation on the expression of neutrophil cytokines modulated by parasite drug susceptibility in CL patients at the onset of disease will contribute to better understand the relationship of these cytokines with the clinical outcome of the infection and/or the treatment.

In addition to chemokine release, here we show that the antimony susceptibility phenotype of the infecting parasite influences the release of other neutrophil cytokines, notably TNF. We detected a decreased production of TNF in the supernatants of human and mouse neutrophils infected with drug-resistant strains compared with those exposed to susceptible strains. Of note, the levels of TNF released by human neutrophils exposed to MA^S parasites were lower than those observed in murine neutrophils. Nevertheless, considering the massive amount of neutrophils recruited to the site of infection, even a low production of TNF on a per cell basis may become physiologically relevant. These results prompted us to investigate the impact of parasite DR in the early TNF release by skin neutrophils in mice infected with the same clinical strains of *L. (V.) panamensis* having distinct susceptibilities to antimonial drug. We showed that infection with drug-resistant parasites resulted in a diminished production of intracellular TNF by neutrophils at the site of infection. Along this line, a decreased parasite survival was reported in N1 neutrophils polarized *in vitro*, which were characterized, among other factors, by a high TNF secretion.[49] TNF production by neutrophils might not only be associated with parasite killing but could also be involved in the autocrine regulation of the release of other cytokines[50] and/or the orchestration of the host immune responses.[51–53]

The traditional view of neutrophils as short-lived cells with limited transcriptional activity and plasticity has been challenged by recent findings using omics technology, particularly single-cell transcriptomics.[26,54–56] These studies unveiled a remarkable diversity in neutrophils in homeostasis and disease[57] and underscored the transcriptional programs of blood neutrophils as a potential main driver of their functional diversification upon stress.[26] In agreement with this, both the study of Ohms et al.[58] and the present results show profound transcriptional changes in human neutrophils upon *Leishmania* infection. Furthermore, here we report for the first time that the transcriptional profile of human neutrophils can be substantially influenced by the parasite susceptibility phenotype for antimonial drug and that their signature is associated with functional outputs. In addition, mapping of the gene expression patterns modulated upon infection with parasites of divergent drug susceptibility onto the most comprehensive transcriptional atlas of human neutrophils to date[26] revealed that the expression of specific genes observed in our study could be restricted to certain neutrophil subpopulations. These data set the stage to further explore scRNA-Seq analyses of *Leishmania*-infected neutrophils *in vitro* and *in situ*.

Remarkably, transcriptional programs elicited by MA^R and MA^S parasites differ greatly in terms of pathways related to immune activation. TLR7 and TLR8 are endosomal TLRs with high homology. Murine neutrophils express TLR7 but not TLR8 whereas human neutrophils express TLR8 but not TLR7.[50,59] *Leishmania* infection triggers TLR7 signaling in murine neutrophils, a process shown to be critical in the control of cutaneous leishmaniasis. Furthermore, *Leishmania*-infected human neutrophils responded to TLR8 agonists similarly than infected mouse neutrophils to TLR7.[60] Given that TLR7/8 signaling has been involved in protective neutrophil responses toward *Leishmania* parasites, we first compared expression patterns triggered by MA^S with a publicly available RNA-Seq dataset of TLR8-activated human neutrophils.[28] This analysis revealed similarities between the corresponding transcriptional patterns. In contrast, infection of neutrophils by MA^R parasites limited the gene expression program reported after TLR8 activation. Using CU-CPT9a, a specific TLR8 antagonist, we show that TLR8 signaling contributes to the higher cytokine release observed in MA^S-infected neutrophils, as inhibition of TLR8 prevented the release of CCL3 and to a lesser extent CXCL8. These results reveal that TLR8 contributes to the mechanisms by which naturally susceptible parasites activate an inflammatory response while naturally resistant parasite dampen this signaling pathway. Recently, SARS-CoV-2 ssRNA was shown to activate human neutrophils in a TLR8-dependent manner, potentially contributing to the pathogenesis of severe disease.[30] Our data show that MA^S parasite stimulation of TLR8 contributes to neutrophil activation and their secretion of cytokine and chemokines attracting myeloid cells.

In line with the transcriptional changes observed between MA^S- and MA^R-infected neutrophils, human neutrophils infected with MA^R parasites are phenotypically less activated than those infected with MA^S parasites. Decreased ROS production, L-selectin shedding, and CD66b expression were previously reported in human neutrophils infected with MA^R parasites compared with those infected with susceptible parasites.[18] Notably, we show here that MA^R parasites upregulated the expression of metallothioneins, molecules that are known to contribute to ROS scavenging and could potentially promote an antioxidant environment that favors parasite persistence.[61]

The higher rates of treatment failure among immunosuppressed leishmaniasis patients[9,62] reinforce the relationship between altered host immunity and the emergence and/or spread of DR. Collectively, our findings unveiled a novel role of neutrophils in the modulation of immune responses during antimony-resistant *Leishmania* infections, which encourages the exploration of neutrophil-targeted approaches to overcome and prevent DR.

Limitations of the study

Our study focused on neutrophil mediators of DR that emerged from transcriptional analyses and were validated at the protein level. However, the correlation of the neutrophil transcriptome with their proteome and/or functional outcome is not always direct,[63,64] and proteomics may reveal other potentially relevant determinants of DR. Several factors may contribute to the different response observed in neutrophils infected with MA^R and MA^s strains. These include host factors, and here, we have focused on neutrophils in host-parasite interactions. The roles of other host cells such as macrophages present in infected skin, as revealed by scRNA-Seq of patient lesions, would provide an integrated view of DR. In addition, one should also consider the importance of parasite diversity between MA^R and MA^S strains and its impact on the differential responses observed in neutrophils. Future work in CL patients will clarify how *in situ* expression of neutrophil mediators involved in DR are associated with clinical outcomes.

STAR★METHODS

Detailed methods are provided in the online version of this paper and include the following:

SUPPLEMENTAL INFORMATION

Supplemental information can be found online at https://doi.org/10.1016/j.isci.2024.109773.

ACKNOWLEDGMENTS

To all patients and healthy donors that participated in this study, to all the members of the FTC Lab for insightful discussions, and to Yazmin Hauyon-La Torre, Florence Prével, and Chantal Desponds for technical assistance. We thank our colleagues in the CIDEIM Jimena Jojoa and Paola Gómez for the isolation of parasites and the development of susceptibility assays and the CIDEIM biobank for technical assistance in *Leishmania* propagation and characterization. We are grateful to Professor Shoumo Bhattacharya from the Radcliffe Department of Medicine & Wellcome Center for Human Genetics of the University of Oxford for the kind gift of Evasin-1 protein and to Professor Renato Ostuni from Vita-Salute San Raffaele University and the San Raffaele Telethon Institute for Gene Therapy (SR-Tiget) for kindly sharing with us the Seurat objects related to the scRNA-Seq data of human neutrophils. We also thank Lausanne Genomic Technologies Facility (GTF), Flow Cytometry Facility (FCF), and Epalinges Animal Facility of the University of Lausanne as well as Transfusion Interrégionale CRS. Funding: this work was supported by the Swiss Program for International Research by Scientific Investigation Teams (SPIRIT) grant of the Swiss National Science Foundation, IZSTZO_190140 to F.T.-C. and N.G.S. and by the United States National Institute of Allergy and Infectious Diseases of the National Institute of Health, TMRC U19AI129910 to N.G.S.

AUTHOR CONTRIBUTIONS

Conceptualization, M.D.-V., N.G.S., and F.T.-C.; methodology, M.D.-V., J.M., O.L.F., N.G.S., and F.T.-C.; formal analysis, M.D.-V. and S.C.-C.; investigation, M.D.-V., A.S.-H., V.T., T.R.S., and L.G.R.; writing—original draft, M.D.-V. and F.T.-C.; writing—review & editing, M.D.-V., A.S.-H., S.C.-C, V.T., T.R.S., J.M., O.L.F., N.G.S., and F.T.-C. All authors have read the manuscript. Funding acquisition, N.G.S. and F.T.-C.

DECLARATION OF INTERESTS

The authors declare no competing interests.

Received: January 9, 2024
Revised: February 22, 2024
Accepted: April 15, 2024
Published: April 18, 2024

REFERENCES

1. World Health Organization (2021). Neglected Tropical Diseases and One Health: Gearing up against Antimicrobial Resistance to Secure the Safety of Future Generations, Meeting Report.
2. Haldar, A.K., Sen, P., and Roy, S. (2011). Use of Antimony in the Treatment of Leishmaniasis: Current Status and Future Directions. Mol. Biol. Int. *2011*, 571242. https://doi.org/10.4061/2011/571242.
3. Rojas, R., Valderrama, L., Valderrama, M., Varona, M.X., Ouellette, M., and Saravia, N.G. (2006). Resistance to Antimony and Treatment Failure in Human Leishmania (Viannia) Infection. J. Infect. Dis. *193*, 1375–1383. https://doi.org/10.1086/503371.
4. eBioMedicine (2023). Leishmania: an urgent need for new treatments. EBioMedicine *87*, 104440. https://doi.org/10.1016/j.ebiom.2023.104440.
5. Ponte-Sucre, A., Gamarro, F., Dujardin, J.-C., Barrett, M.P., López-Vélez, R., García-Hernández, R., Pountain, A.W., Mwenechanya, R., and Papadopoulou, B. (2017). Drug resistance and treatment failure in leishmaniasis: A 21st century challenge. PLoS Negl. Trop. Dis. *11*, e0006052. https://doi.org/10.1371/journal.pntd.0006052.
6. Domagalska, M.A., Barrett, M.P., and Dujardin, J.-C. (2023). Drug resistance in Leishmania: does it really matter? Trends Parasitol. *39*, 251–259. https://doi.org/10.1016/j.pt.2023.01.012.
7. Fernández, O.L., Diaz-Toro, Y., Ovalle, C., Valderrama, L., Muvdi, S., Rodríguez, I., Gomez, M.A., and Saravia, N.G. (2014). Miltefosine and Antimonial Drug Susceptibility of Leishmania Viannia Species and Populations in Regions of High Transmission in Colombia. PLoS Negl. Trop. Dis. *8*, e2871. https://doi.org/10.1371/journal.pntd.0002871.
8. Gutierrez, Y., Salinas, G.H., Palma, G., Valderrama, L.B., Santrich, C.V., and Saravia, N.G. (1991). Correlation between Histopathology, Immune Response, Clinical Presentation, and Evolution in Leishmania braziliensis Infection. Am. J. Trop. Med. Hyg. *45*, 281–289. https://doi.org/10.4269/ajtmh.1991.45.281.
9. Alvar, J., Cañavate, C., Gutiérrez-Solar, B., Jiménez, M., Laguna, F., López-Vélez, R., Molina, R., and Moreno, J. (1997). Leishmania and human immunodeficiency virus coinfection: The first 10 years. Clin. Microbiol. Rev. *10*, 298–319. https://doi.org/10.1128/cmr.10.2.298.
10. Dalton, J.E., and Kaye, P.M. (2010). Immunomodulators: use in combined therapy against leishmaniasis. Expert Rev. Anti Infect. Ther. *8*, 739–742. https://doi.org/10.1586/eri.10.64.
11. Passelli, K., Billion, O., and Tacchini-Cottier, F. (2021). The Impact of Neutrophil Recruitment to the Skin on the Pathology Induced by Leishmania Infection. Front. Immunol. *12*, 649348. https://doi.org/10.3389/fimmu.2021.649348.
12. Ley, K., Hoffman, H.M., Kubes, P., Cassatella, M.A., Zychlinsky, A., Hedrick, C.C., and Catz, S.D. (2018). Neutrophils: New insights and open questions. Sci. Immunol. *3*, eaat4579. https://doi.org/10.1126/sciimmunol.aat4579.
13. Burn, G.L., Foti, A., Marsman, G., Patel, D.F., and Zychlinsky, A. (2021). The Neutrophil. Immunity *54*, 1377–1391. https://doi.org/10.1016/j.immuni.2021.06.006.
14. Mantovani, A., Cassatella, M.A., Costantini, C., and Jaillon, S. (2011). Neutrophils in the activation and regulation of innate and adaptive immunity. Nat. Rev. Immunol. *11*, 519–531. https://doi.org/10.1038/nri3024.
15. Cassatella, M.A., Östberg, N.K., Tamassia, N., and Soehnlein, O. (2019). Biological Roles of Neutrophil-Derived Granule Proteins and Cytokines. Trends Immunol. *40*, 648–664. https://doi.org/10.1016/j.it.2019.05.003.
16. Regli, I.B., Passelli, K., Hurrell, B.P., and Tacchini-Cottier, F. (2017). Survival mechanisms used by some Leishmania species to escape neutrophil killing. Front. Immunol. *8*, 1558. https://doi.org/10.3389/fimmu.2017.01558.
17. Regli, I.B., Fernández, O.L., Martínez-Salazar, B., Gómez, M.A., Saravia, N.G., and Tacchini-Cottier, F. (2018). Resistance of Leishmania (Viannia) Panamensis to Meglumine Antimoniate or Miltefosine Modulates Neutrophil Effector Functions. Front. Immunol. *9*, 3040. https://doi.org/10.3389/fimmu.2018.03040.
18. Fernández, O.L., Ramírez, L.G., Díaz-Varela, M., Tacchini-Cottier, F., and Saravia, N.G. (2021). Neutrophil Activation: Influence of Antimony Tolerant and Susceptible Clinical Strains of L. (V.) panamensis and Meglumine Antimoniate. Front. Cell. Infect. Microbiol. *11*, 710006. https://doi.org/10.3389/fcimb.2021.710006.
19. Saravia, N.G., Weigle, K., Navas, C., Segura, I., Valderrama, L., Valencia, A.Z., Escorcia, B., and McMahon-Pratt, D. (2002). Heterogeneity, geographic distribution, and pathogenicity of serodemes of Leishmania viannia in Colombia. Am. J. Trop. Med. Hyg. *66*, 738–744. https://doi.org/10.4269/ajtmh.2002.66.738.
20. Saravia, N.G., Segura, I., Holguin, A.F., Santrich, C., Valderrama, L., and Ocampo, C. (1998). Epidemiologic, genetic, and clinical associations among phenotypically distinct populations of Leishmania (Viannia) in Colombia. Am. J. Trop. Med. Hyg. *59*, 86–94. https://doi.org/10.4269/ajtmh.1998.59.86.
21. Fernández, O., Diaz-Toro, Y., Valderrama, L., Ovalle, C., Valderrama, M., Castillo, H., Perez, M., and Saravia, N.G. (2012). Novel Approach to In Vitro Drug Susceptibility Assessment of Clinical Strains of Leishmania spp. J. Clin. Microbiol. *50*, 2207–2211. https://doi.org/10.1128/JCM.00216-12.
22. Subramanian, A., Tamayo, P., Mootha, V.K., Mukherjee, S., Ebert, B.L., Gillette, M.A., Paulovich, A., Pomeroy, S.L., Golub, T.R., Lander, E.S., and Mesirov, J.P. (2005). Gene set enrichment analysis: A knowledge-based approach for interpreting genome-wide expression profiles. Proc. Natl. Acad. Sci. USA *102*, 15545–15550. https://doi.org/10.1073/PNAS.0506580102.
23. Liberzon, A., Birger, C., Thorvaldsdóttir, H., Ghandi, M., Mesirov, J.P., and Tamayo, P. (2015). The Molecular Signatures Database Hallmark Gene Set Collection. Cell Syst. *1*, 417–425. https://doi.org/10.1016/j.cels.2015.12.004.
24. Vallee, B.L. (1995). The function of metallothionein. Neurochem. Int. *27*, 23–33. https://doi.org/10.1016/0197-0186(94)00165-Q.
25. Coyle, P., Philcox, J.C., Carey, L.C., and Rofe, A.M. (2002). Metallothionein: the multipurpose protein. Cell. Mol. Life Sci. *59*, 627–647. https://doi.org/10.1007/s00018-002-8454-2.
26. Montaldo, E., Lusito, E., Bianchessi, V., Caronni, N., Scala, S., Basso-Ricci, L., Cantaffa, C., Masserdotti, A., Barilaro, M., Barresi, S., et al. (2022). Cellular and transcriptional dynamics of human neutrophils at steady state and upon stress. Nat. Immunol. *23*, 1470–1483. https://doi.org/10.1038/s41590-022-01311-1.
27. Deniset, J.F., and Kubes, P. (2018). Neutrophil heterogeneity: Bona fide subsets or polarization states? J. Leukoc. Biol. *103*, 829–838. https://doi.org/10.1002/JLB.3RI0917-361R.
28. Tamassia, N., Bianchetto-Aguilera, F., Gasperini, S., Polletti, S., Gardiman, E., Ostuni, R., Natoli, G., and Cassatella, M.A. (2021). Induction of OCT2 contributes to regulate the gene expression program in human neutrophils activated via TLR8. Cell Rep. *35*, 109143. https://doi.org/10.1016/j.celrep.2021.109143.
29. Frauenschuh, A., Power, C.A., Déruaz, M., Ferreira, B.R., Silva, J.S., Teixeira, M.M., Dias, J.M., Martin, T., Wells, T.N.C., and Proudfoot, A.E.I. (2007). Molecular Cloning and Characterization of a Highly Selective Chemokine-binding Protein from the Tick Rhipicephalus sanguineus. J. Biol. Chem. *282*, 27250–27258. https://doi.org/10.1074/jbc.M704706200.
30. Gardiman, E., Bianchetto-Aguilera, F., Gasperini, S., Tiberio, L., Scandola, M., Lotti, V., Gibellini, D., Salvi, V., Bosisio, D., Cassatella, M.A., and Tamassia, N. (2022). SARS-CoV-2-Associated ssRNAs Activate Human Neutrophils in a TLR8-Dependent Fashion. Cells *11*, 3785. https://doi.org/10.3390/cells11233785.
31. Muñoz-Durango, N., Gómez, A., García-Valencia, N., Roldán, M., Ochoa, M., Bautista-Erazo, D.E., and Ramírez-Pineda, J.R. (2022). A Mouse Model of Ulcerative Cutaneous Leishmaniasis by Leishmania (Viannia) panamensis to Investigate Infection, Pathogenesis, Immunity, and Therapeutics. Front. Microbiol. *13*, 907631. https://doi.org/10.3389/fmicb.2022.907631.
32. Tacchini-Cottier, F., Zweifel, C., Belkaid, Y., Mukankundiye, C., Vasei, M., Launois, P., Milon, G., and Louis, J.A. (2000). An immunomodulatory function for neutrophils during the induction of a CD4+ Th2 response in BALB/c mice infected with Leishmania major. J. Immunol. *165*, 2628–2636. https://doi.org/10.4049/JIMMUNOL.165.5.2628.
33. Peters, N.C., Egen, J.G., Secundino, N., Debrabant, A., Kimblin, N., Kamhawi, S., Lawyer, P., Fay, M.P., Germain, R.N., and Sacks, D. (2008). In vivo imaging reveals an essential role for neutrophils in leishmaniasis transmitted by sand flies. Science *321*, 970–974. https://doi.org/10.1126/science.1159194.
34. Ribeiro-Gomes, F.L., Roma, E.H., Carneiro, M.B.H., Doria, N.A., Sacks, D.L., and Peters, N.C. (2014). Site-dependent recruitment of inflammatory cells determines the effective dose of Leishmania major. Infect. Immun. *82*, 2713–2727. https://doi.org/10.1128/IAI.01600-13.
35. Hurrell, B.P., Schuster, S., Grün, E., Coutaz, M., Williams, R.A., Held, W., Malissen, B., Malissen, M., Yousefi, S., Simon, H.U., et al. (2015). Rapid Sequestration of Leishmania mexicana by Neutrophils Contributes to the

Development of Chronic Lesion. PLoS Pathog. *11*, e1004929. https://doi.org/10.1371/journal.ppat.1004929.

36. Prat-Luri, B., Neal, C., Passelli, K., Ganga, E., Amore, J., Firmino-Cruz, L., Petrova, T.V., Müller, A.J., and Tacchini-Cottier, F. (2022). The C5a-C5aR1 complement axis is essential for neutrophil recruitment to draining lymph nodes via high endothelial venules in cutaneous leishmaniasis. Cell Rep. *39*, 110777. https://doi.org/10.1016/j.celrep.2022.110777.
37. Charmoy, M., Brunner-Agten, S., Aebischer, D., Auderset, F., Launois, P., Milon, G., Proudfoot, A.E.I., and Tacchini-Cottier, F. (2010). Neutrophil-Derived CCL3 Is Essential for the Rapid Recruitment of Dendritic Cells to the Site of Leishmania major Inoculation in Resistant Mice. PLoS Pathog. *6*, e1000755. https://doi.org/10.1371/journal.ppat.1000755.
38. Tecchio, C., and Cassatella, M.A. (2016). Neutrophil-derived chemokines on the road to immunity. Semin. Immunol. *28*, 119–128. https://doi.org/10.1016/j.smim.2016.04.003.
39. Jiang, J.H., Bhuiyan, M.S., Shen, H.H., Cameron, D.R., Rupasinghe, T.W.T., Wu, C.M., Le Brun, A.P., Kostoulias, X., Domene, C., Fulcher, A.J., et al. (2019). Antibiotic resistance and host immune evasion in Staphylococcus aureus mediated by a metabolic adaptation. Proc. Natl. Acad. Sci. USA *116*, 3722–3727. https://doi.org/10.1073/pnas.1812066116.
40. Zwack, E.E., Chen, Z., Devlin, J.C., Li, Z., Zheng, X., Weinstock, A., Lacey, K.A., Fisher, E.A., Fenyö, D., Ruggles, K.V., et al. (2022). Staphylococcus aureus induces a muted host response in human blood that blunts the recruitment of neutrophils. Proc. Natl. Acad. Sci. USA *119*, e2123017119. https://doi.org/10.1073/pnas.2123017119.
41. Bulté, D., Van Bockstal, L., Dirkx, L., Van den Kerkhof, M., De Trez, C., Timmermans, J.-P., Hendrickx, S., Maes, L., and Caljon, G. (2021). Miltefosine enhances infectivity of a miltefosine-resistant Leishmania infantum strain by attenuating its innate immune recognition. PLoS Negl. Trop. Dis. *15*, e0009622. https://doi.org/10.1371/journal.pntd.0009622.
42. Mukherjee, B., Mukhopadhyay, R., Bannerjee, B., Chowdhury, S., Mukherjee, S., Naskar, K., Allam, U.S., Chakravortty, D., Sundar, S., Dujardin, J.-C., and Roy, S. (2013). Antimony-resistant but not antimony-sensitive Leishmania donovani up-regulates host IL-10 to overexpress multidrug-resistant protein 1. Proc. Natl. Acad. Sci. USA *110*, E575–E582. https://doi.org/10.1073/pnas.1213839110.
43. Haldar, A.K., Yadav, V., Singhal, E., Bisht, K.K., Singh, A., Bhaumik, S., Basu, R., Sen, P., and Roy, S. (2010). Leishmania donovani Isolates with Antimony-Resistant but Not -Sensitive Phenotype Inhibit Sodium Antimony Gluconate-Induced Dendritic Cell Activation. PLoS Pathog. *6*, e1000907. https://doi.org/10.1371/journal.ppat.1000907.
44. Guha, R., Das, S., Ghosh, J., Sundar, S., Dujardin, J.C., and Roy, S. (2014). Antimony Resistant Leishmania donovani but Not Sensitive Ones Drives Greater Frequency of Potent T-Regulatory Cells upon Interaction with Human PBMCs: Role of IL-10 and TGF-β in Early Immune Response. PLoS Negl. Trop. Dis. *8*, e2995. https://doi.org/10.1371/journal.pntd.0002995.
45. Bhattacharya, P., Ismail, N., Saxena, A., Gannavaram, S., Dey, R., Oljuskin, T., Akue, A., Takeda, K., Yu, J., Karmakar, S., et al. (2022). Neutrophil-dendritic cell interaction plays an important role in live attenuated Leishmania vaccine induced immunity. PLoS Negl. Trop. Dis. *16*, e0010224. https://doi.org/10.1371/journal.pntd.0010224.
46. Fernández O.L., Rosales-Chilama M., Sánchez-Hidalgo A., Gomez P., Rebellón-Sánchez D.E., Regli I.B., Díaz-Varela M., Tacchini-Cottier F., Saravia N. G. Natural resistance to meglumine antimoniate is associated with treatment failure in cutaneous leishmaniasis caused by *Leishmania* (*Viannia*) *panamensis*. PLoS Negl. Trop. Dis. 2024; *in press*
47. Navas, A., Vargas, D.A., Freudzon, M., McMahon-Pratt, D., Saravia, N.G., and Gómez, M.A. (2014). Chronicity of Dermal Leishmaniasis Caused by Leishmania panamensis Is Associated with Parasite-Mediated Induction of Chemokine Gene Expression. Infect. Immun. *82*, 2872–2880. https://doi.org/10.1128/IAI.01133-13.
48. Navas, A., Fernández, O., Gallego-Marín, C., Castro, M.D.M., Rosales-Chilama, M., Murillo, J., Cossio, A., McMahon-Pratt, D., Saravia, N.G., and Gómez, M.A. (2020). Profiles of Local and Systemic Inflammation in the Outcome of Treatment of Human Cutaneous Leishmaniasis Caused by Leishmania (Viannia). Infect. Immun. *88*, e00764-19. https://doi.org/10.1128/IAI.00764-19.
49. Ohms, M., Möller, S., and Laskay, T. (2020). An Attempt to Polarize Human Neutrophils Toward N1 and N2 Phenotypes *in vitro*. Front. Immunol. *11*, 532–612. https://doi.org/10.3389/fimmu.2020.00532.
50. Zimmermann, M., Aguilera, F.B., Castellucci, M., Rossato, M., Costa, S., Lunardi, C., Ostuni, R., Girolomoni, G., Natoli, G., Bazzoni, F., et al. (2015). Chromatin remodelling and autocrine TNFα are required for optimal interleukin-6 expression in activated human neutrophils. Nat. Commun. *6*, 6061. https://doi.org/10.1038/ncomms7061.
51. Bennouna, S., Bliss, S.K., Curiel, T.J., and Denkers, E.Y. (2003). Cross-Talk in the Innate Immune System: Neutrophils Instruct Recruitment and Activation of Dendritic Cells during Microbial Infection. J. Immunol. *171*, 6052–6058. https://doi.org/10.4049/jimmunol.171.11.6052.
52. Van Gisbergen, K.P.J.M., Sanchez-Hernandez, M., Geijtenbeek, T.B.H., and Van Kooyk, Y. (2005). Neutrophils mediate immune modulation of dendritic cells through glycosylation-dependent interactions between Mac-1 and DC-SIGN. J. Exp. Med. *201*, 1281–1292. https://doi.org/10.1084/jem.20041276.
53. Youn, C., Pontaza, C., Wang, Y., Dikeman, D.A., Joyce, D.P., Alphonse, M.P., Wu, M.-J., Nolan, S.J., Anany, M.A., Ahmadi, M., et al. (2023). Neutrophil-intrinsic TNF receptor signaling orchestrates host defense against Staphylococcus aureus. Sci. Adv. *9*. eadf8748–18. https://doi.org/10.1126/sciadv.adf8748.
54. Ballesteros, I., Rubio-Ponce, A., Genua, M., Lusito, E., Kwok, I., Fernández-Calvo, G., Khoyratty, T.E., van Grinsven, E., González-Hernández, S., Nicolás-Ávila, J.Á., et al. (2020). Co-option of Neutrophil Fates by Tissue Environments. Cell *183*, 1282–1297.e18. https://doi.org/10.1016/j.cell.2020.10.003.
55. Xie, X., Shi, Q., Wu, P., Zhang, X., Kambara, H., Su, J., Yu, H., Park, S.-Y., Guo, R., Ren, Q., et al. (2020). Single-cell transcriptome profiling reveals neutrophil heterogeneity in homeostasis and infection. Nat. Immunol. *21*, 1119–1133. https://doi.org/10.1038/s41590-020-0736-z.
56. Grieshaber-Bouyer, R., Radtke, F.A., Cunin, P., Stifano, G., Levescot, A., Vijaykumar, B., Nelson-Maney, N., Blaustein, R.B., Monach, P.A., and Nigrovic, P.A.; ImmGen Consortium (2021). The neutrotime transcriptional signature defines a single continuum of neutrophils across biological compartments. Nat. Commun. *12*, 2856. https://doi.org/10.1038/s41467-021-22973-9.
57. Palomino-Segura, M., Sicilia, J., Ballesteros, I., and Hidalgo, A. (2023). Strategies of neutrophil diversification. Nat. Immunol. *24*, 575–584. https://doi.org/10.1038/s41590-023-01452-x.
58. Ohms, M., Ferreira, C., Busch, H., Wohlers, I., Guerra de Souza, A.C., Silvestre, R., and Laskay, T. (2021). Enhanced Glycolysis Is Required for Antileishmanial Functions of Neutrophils Upon Infection With Leishmania donovani. Front. Immunol. *12*, 632512. https://doi.org/10.3389/fimmu.2021.632512.
59. Liu, J., Xu, C., Hsu, L.-C., Luo, Y., Xiang, R., and Chuang, T.-H. (2010). A five-amino-acid motif in the undefined region of the TLR8 ectodomain is required for species-specific ligand recognition. Mol. Immunol. *47*, 1083–1090. https://doi.org/10.1016/j.molimm.2009.11.003.
60. Regli, I.B., Passelli, K., Martínez-Salazar, B., Amore, J., Hurrell, B.P., Müller, A.J., and Tacchini-Cottier, F. (2020). TLR7 Sensing by Neutrophils Is Critical for the Control of Cutaneous Leishmaniasis. Cell Rep. *31*, 107746. https://doi.org/10.1016/j.celrep.2020.107746.
61. Ruttkay-Nedecky, B., Nejdl, L., Gumulec, J., Zitka, O., Masarik, M., Eckschlager, T., Stiborova, M., Adam, V., and Kizek, R. (2013). The Role of Metallothionein in Oxidative Stress. Int. J. Mol. Sci. *14*, 6044–6066. https://doi.org/10.3390/ijms14036044.
62. Cojean, S., Houzé, S., Haouchine, D., Huteau, F., Lariven, S., Hubert, V., Michard, F., Bories, C., Pratlong, F., le Bras, J., et al. (2012). Leishmania Resistance to Miltefosine Associated with Genetic Marker. Emerg. Infect. Dis. *18*, 704–706. https://doi.org/10.3201/EID1804.110841.
63. Hoogendijk, A.J., Pourfarzad, F., Aarts, C.E.M., Tool, A.T.J., Hiemstra, I.H., Grassi, L., Frontini, M., Meijer, A.B., van den Biggelaar, M., and Kuijpers, T.W. (2019). Dynamic Transcriptome-Proteome Correlation Networks Reveal Human Myeloid Differentiation and Neutrophil-Specific Programming. Cell Rep. *29*, 2505–2519.e4. https://doi.org/10.1016/j.celrep.2019.10.082.
64. Adrover, J.M., Aroca-Crevillén, A., Crainiciuc, G., Ostos, F., Rojas-Vega, Y., Rubio-Ponce, A., Cilloniz, C., Bonzón-Kulichenko, E., Calvo, E., Rico, D., et al. (2020). Programmed 'disarming' of the neutrophil proteome reduces the magnitude of inflammation. Nat. Immunol. *21*, 135–144. https://doi.org/10.1038/s41590-019-0571-2.
65. Martin, M. (2011). Cutadapt removes adapter sequences from high-throughput sequencing reads. EMBnet. J. *17*, 10–12. https://doi.org/10.14806/EJ.17.1.200.
66. Wingett, S.W., and Andrews, S. (2018). FastQ Screen: A tool for multi-genome mapping and quality control. F1000Res. *7*, 1338. https://doi.org/10.12688/F1000RESEARCH.15931.2.

67. Davis, M.P.A., van Dongen, S., Abreu-Goodger, C., Bartonicek, N., and Enright, A.J. (2013). Kraken: a set of tools for quality control and analysis of high-throughput sequence data. Methods *63*, 41–49. https://doi.org/10.1016/J.YMETH.2013.06.027.

68. Dobin, A., Davis, C.A., Schlesinger, F., Drenkow, J., Zaleski, C., Jha, S., Batut, P., Chaisson, M., and Gingeras, T.R. (2013). STAR: ultrafast universal RNA-seq aligner. Bioinformatics *29*, 15–21. https://doi.org/10.1093/BIOINFORMATICS/BTS635.

69. Anders, S., Pyl, P.T., and Huber, W. (2015). HTSeq—a Python framework to work with high-throughput sequencing data. Bioinformatics *31*, 166–169. https://doi.org/10.1093/BIOINFORMATICS/BTU638.

70. Ritchie, M.E., Phipson, B., Wu, D., Hu, Y., Law, C.W., Shi, W., and Smyth, G.K. (2015). limma powers differential expression analyses for RNA-sequencing and microarray studies. Nucleic Acids Res. *43*, e47. https://doi.org/10.1093/NAR/GKV007.

71. Stuart, T., Butler, A., Hoffman, P., Hafemeister, C., Papalexi, E., Mauck, W.M., Hao, Y., Stoeckius, M., Smibert, P., and Satija, R. (2019). Comprehensive Integration of Single-Cell Data. Cell *177*, 1888–1902.e21. https://doi.org/10.1016/J.CELL.2019.05.031.

72. Wu, T., Hu, E., Xu, S., Chen, M., Guo, P., Dai, Z., Feng, T., Zhou, L., Tang, W., Zhan, L., et al. (2021). clusterProfiler 4.0: A universal enrichment tool for interpreting omics data. Innovation *2*, 100141. https://doi.org/10.1016/J.XINN.2021.100141.

73. Yu, G., Wang, L.G., Han, Y., and He, Q.Y. (2012). clusterProfiler: an R package for comparing biological themes among gene clusters. OMICS *16*, 284–287. https://doi.org/10.1089/OMI.2011.0118.

74. Passelli, K., Prat-Luri, B., Merlot, M., Goris, M., Mazzone, M., and Tacchini-Cottier, F. (2022). The c-MET receptor tyrosine kinase contributes to neutrophil-driven pathology in cutaneous leishmaniasis. PLoS Pathog. *18*, e1010247. https://doi.org/10.1371/journal.ppat.1010247.

75. Hao, Y., Hao, S., Andersen-Nissen, E., Mauck, W.M., Zheng, S., Butler, A., Lee, M.J., Wilk, A.J., Darby, C., Zager, M., et al. (2021). Integrated analysis of multimodal single-cell data. Cell *184*, 3573–3587.e29. https://doi.org/10.1016/J.CELL.2021.04.048.

STAR★METHODS

KEY RESOURCES TABLE

REAGENT or RESOURCE	SOURCE	IDENTIFIER
Antibodies		
Anti-human CD45-PE/eFluor 610	Invitrogen	Cat#61-0459-42; RRID:AB_2574566
Anti-human CD15-APC	Invitrogen	Cat#17-0158-42; RRID: AB_2573137
Anti-human CD14-PE	Invitrogen	Cat#MHCD1404; RRID: AB_10373109
Anti-mouse CD45-PerCP/Cy5.5	BD Biosciences	Cat#550994; RRID: AB_394003
Anti-mouse Ly6C-FITC	BD Biosciences	Cat#553104; RRID: AB_394628
Anti-mouse Ly6G-APC/Cy7	Biolegend	Cat#127624; RRID: AB_10640819
Anti-mouse CD11b-BV605	BD Biosciences	Cat#563015; RRID: AB_2737951
Anti-mouse CD11c-PE	Invitrogen	Cat#12-0114-83; RRID: AB_465553
Anti-mouse CD206- PE/Cy7	Biolegend	Cat#141719; RRID: AB_2562247
Anti-mouse SiglecF-BUV395	BD Biosciences	Cat#740280; RRID: AB_2740019
Anti-mouse TNF-APC	BD Biosciences	Cat#554420; RRID: AB_398553
Human IL-8/CXCL8 Antibody	R&D Systems	Cat#MAB208; RRID: AB_2249110
Mouse IgG1 Isotype Control	R&D Systems	Cat#MAB002; RRID: AB_357344
Biological samples		
Healthy donor blood	Transfusion Interrégionale CRS, Epalinges, Switzerland	N/A
Healthy donor blood	CIDEIM, Cali, Colombia	N/A
Chemicals, peptides, and recombinant proteins		
Polymorphprep	Alere Technologies AS	Cat#1114683
TheraPEAK™ ACK Lysing Buffer	Lonza	Cat#BP10-548E
Diff-Quick RAL 555	RAL Diagnostics	Cat#381550-0000
Human AB serum	Sigma	Cat#H4522
Fetal Bovine Serum	Gibco	Cat#10270-106
Recombinant Human CCL3/MIP-1 alpha Protein	R&D Systems	Cat# 270-LD
Recombinant Evasin-1 Protein	Frauenschuh et al.[29] Gift from Prof. Shoumo Bhattacharya, University of Oxford, United Kingdom	https://doi.org/10.1074/jbc.m704706200
Meglumine Antimoniate	Walter Reed	Cat#*214975AK*
Albumin (BSA)	ITW Reagents	Cat#A1391
N-Formyl-L-methionyl-L-leucyl-L-phenylalanine (fMLP)	Sigma	Cat#F3506
Phorbol-12-myristate-13-acetate (PMA)	Sigma	Cat#P1585
Diphenyleneiodonium chloride (DPI)	Sigma	Cat#D2926
Luminol	Sigma	Cat#09253
Resiquimod (R848)	InvivoGen	Cat#Tlrl-r848
CU-CPT9a TLR8 inhibitor - InvitroFit™	InvivoGen	Cat#Inh-cc9a
Liberase TL	Roche	Cat#250850
Golgi Plug Protein Transport Inhibitor	BD Biosciences	Cat#555029
Fixation and Permeabilization Buffer Set	Invitrogen	Cat#00-5523-00
RPMI medium 1640	Gibco	Cat#61870-010
X-VIVO™ medium	Lonza	Cat#BEBP02-061Q

(*Continued on next page*)

Continued

REAGENT or RESOURCE	SOURCE	IDENTIFIER
Critical commercial assays		
EasySep™ Human Neutrophil Isolation Kit	STEMCELL Technologies	Cat#17957
EasySep™ Human CD14 Positive Selection Kit II	STEMCELL Technologies	Cat#17858
Neutrophil Isolation Kit mouse	Miltenyi Biotec	Cat#130-097-658
LIVE/DEAD Fixable Aqua dead Cell Stain kit	Invitrogen	Cat#L34957
RNeasy Plus Mini Kit	Qiagen	Cat#74134
High-Capacity cDNA Reverse Transcription Kit	Applied Biosystems™	Cat#4368814
QIAquick PCR purification Kit	Qiagen	Cat#28104
LightCycler 480 SYBR Green I Master	Roche	Cat#04887352001
SMART-Seq® v4 PLUS Kit	Takara	Cat#R400752
SPRISelect beads	Beckman Coulter	Cat#B23319
Qubit™ RNA High Sensitivity (HS)	ThermoFisher Scientific	Cat#Q32852
Quant-iT™ PicoGreen™ dsDNA Assay	ThermoFisher Scientific	Cat#P7589
NGS Fragment Kit (1-6000bp)	Agilent Technologies	Cat#NF-473-0500
NovaSeq 6000 S1 Reagent Kit v1.5 (100 cycles)	Illumina	Cat#20028319
Human ProcartaPlex™ Mix & Match 13-plex	Thermo Fisher	Cat#PPX-13-MXH6CD2
SYBR Green PCR Master Mix	Applied biosystems	Cat#4309155
Mouse TNF alpha DuoSet ELISA	R&D Systems	Cat#DY410
Mouse MIP-1 alpha Uncoated ELISA Kit	Invitrogen	Cat#88-56013-88
Mouse CXCL2/MIP-2 DuoSet ELISA	R&D Systems	Cat#DY452
Mouse CXCL1/KC DuoSet ELISA	R&D Systems	Cat#DY453
Human IL-8/CXCL8 DuoSet ELISA	R&D Systems	Cat#DY208
Human CCL3 (MIP-1 alpha) Uncoated ELISA	Invitrogen	Cat#88-7035
Deposited data		
RNA-Seq data	This paper	GEO Accession: GSE244972
Single-cell RNA-Seq data of human neutrophils	Montaldo et al.[26]	ArrayExpress: E-MTAB-11188
Experimental models: Organisms/strains		
Parasite strains of *Leishmania (Viannia) panamensis*, see Table S1	CIDEIM Biobank	
Mouse: BALB/cOlaHsd	Envigo/Inotiv	https://www.inotivco.com/model/balb-colahsd
Oligonucleotides		
Primers for RT-qPCR, see Table S3	Microsynth	N/A
Software and algorithms		
Bcl2fastq2 Conversion Software v. 2.20	Illumina	https://emea.support.illumina.com/downloads/bcl2fastq-conversion-software-v2-20.html
Cutadapt v. 2.5	Martin[65]	https://doi.org/10.14806/ej.17.1.200
Fastq_screen v. 0.11.1	Wingett and Andrews[66]	https://doi.org/10.12688/f1000research.15931.2
Reaper v. 15-065	Davis et al.[67]	https://doi.org/10.1016/j.ymeth.2013.06.027
STAR v. 2.5.3a	Dobin et al.[68]	https://doi.org/10.1093/bioinformatics/bts635
Htseq v. 0.9.1	Anders et al.[69]	https://doi.org/10.1093/bioinformatics/btu638
R v. 4.1.1 and v. 4.3.0	R Core Team, 2022	https://www.R-project.org
Limma v. 3.48.3	Ritchie et al.[70]	https://doi.org/10.1093/nar/gkv007
Seurat v. 4.3.0	Stuart et al.[71]	https://doi.org/10.1016/j.cell.2019.05.031

(*Continued on next page*)

Continued

REAGENT or RESOURCE	SOURCE	IDENTIFIER
clusterProfiler v. 4.0.5	Wu et al.[72] Yu et al.[73]	https://doi.org/10.1016/j.xinn.2021.100141 https://doi.org/10.1089/omi.2011.0118
FlowJo, v. 10.9.0	Becton Dickinson & Company (BD)	https://www.flowjo.com/
GraphPad Prism v. 9.5.1	GraphPad Prism	https://www.graphpad.com/
Bio-Plex Manager™ Software v. 6.2	Bio-Rad	https://www.bio-rad.com/en-ch/product/bio-plex-manager-software-standard-edition

RESOURCE AVAILABILITY

Lead contact

Further information and requests for resources and reagents should be directed to and will be fulfilled by the lead contact, Fabienne Tacchini-Cottier (Fabienne.Tacchini-Cottier@unil.ch).

Materials availability

This study did not generate new unique reagents.

Data and code availability

- RNA-Seq data have been deposited at GEO and are publicly available as of the date of publication. This paper analyzes existing, publicly available single-cell RNA-Seq data. Accession numbers for the datasets are listed in the key resources table. Additional data reported in this paper will be shared by the lead contact upon request.
- This paper does not report original code.
- Any additional information required to reanalyze the data reported in this paper is available from the lead contact upon request.

EXPERIMENTAL MODEL AND STUDY PARTICIPANT DETAILS

Human subjects

Thirteen healthy human blood donors without history of leishmaniasis participated in this study (8 females and 5 males and, 23-57 years old). All study procedures were approved by the by the Ethical Committees of the Canton of Vaud (CER-VD2017-00182) and the Centro Internacional de Entrenamiento e Investigaciones Médicas (CIDEIM) (Approval CEIH code: 1303) and were conducted in compliance with the legislation of the Canton of Vaud and the Swiss Confederation as well as the Declaration of Helsinki. Written informed consent was obtained from all volunteers.

Mice

Male and female BALB/c mice were purchased from Envigo (Cambridgeshire, United Kingdom). Mice were housed at the animal facility of the University of Lausanne in Epalinges under pathogen-free conditions and used for experiments at 6-7 weeks of age. Animal experimentation protocols were approved by the veterinary office of the Canton of Vaud (Authorizations 3476x1a and 3616b and to F.T.-C.) and were performed in accordance to cantonal and federal law as well as the principles of the declaration of Basel.

Leishmania (Viannia) panamensis clinical strains

Clinical strains of *L. (V.) panamensis* isolated from cutaneous leishmaniasis patients and previously defined as susceptible or resistant to MA were obtained from the CIDEIM Biobank. Susceptibility of parasites to MA was determined as reduction of intracellular *Leishmania* amastigote burden in U-937 macrophages as previously described.[21] Susceptibility to pentavalent antimony (32 μg Sb^V/mL) as MA, zymodeme and symbol of each strain included in the study are described in Table S1. For experimental infections, promastigotes of *Leishmania* strains were propagated in culture at 25°C in Senejke's diphasic blood agar medium with PBS for six days. Promastigotes were opsonized for 60 min at 37°C in 10% human AB serum (Sigma) or 10% naïve mouse serum prior to exposure to human or murine neutrophils, respectively. Unopsonized stationary promastigotes were used for *in vivo* infections.

METHOD DETAILS

Isolation of cells

Human neutrophils were isolated from the venous blood of healthy donors collected in heparinized tubes. Neutrophils were purified upon density gradient centrifugation using polymorphprep (Alere Technologies AS) and remaining red blood cells were lysed using TheraPEAK™ ACK Lysing Buffer (Lonza) according to the manufacturer's instructions. For RNA-Seq, qPCR and ELISA, enriched neutrophils were further

subjected to negative isolation using the EasySep™ Human Neutrophil Isolation Kit (STEMCELL Technologies) following manufacturer's indications in order to ensure > 99% purity. Human $CD14^+$-monocytes were isolated from PBMC fraction obtained by density gradient centrifugation with polymorphprep (Alere Technologies AS) using the by EasySep™ Human CD14 Isolation Kit (STEMCELL Technologies) following manufacturer's instructions to reach > 98% purity. Human neutrophil and monocyte purity was monitored by cytospin and Diff-Quick staining (RAL Diagnostics) as well as by analysis using an LSRFortessa flow cytometer (BD Biosciences) and FlowJo software (BD) after staining with anti-human CD45 (HI30)-PE/eFluor 610, anti-human CD15 (MMA) -APC and Live/Dead fixable Aqua Dead Cell Stain Kit (Invitrogen) for human neutrophils, and staining with anti-human CD14 (TuK4)-PE for human monocytes. Murine neutrophils were isolated from the bone marrow (BM) of naïve mice. Femora and tibia were collected and BM was obtained by centrifugation. Neutrophils were purified by negative magnetic-activated cells sorting using the Neutrophil Isolation Kit (Miltenyi Biotec) according to the manufacturer's instructions. The purity of murine neutrophils (>95%) was assessed by cytospin and Diff-Quick staining (RAL Diagnostics).

RNA isolation from *ex vivo* infected neutrophils

Purified human neutrophils were cultured in RPMI-1640 medium (Gibco) supplemented with 2% HI human AB serum (Sigma) (2.5×10^6 cells/mL) in the presence or absence of *L. (V.) panamensis* parasites at a multiplicity of infection (MOI) of 2 for 6 h. Neutrophils were then lysed in RLT buffer and immediately snap-frozen. RNA was extracted using the RNeasy Plus Mini Kit (Qiagen) according to manufacturer's instructions. RNA concentration and quality were determined by a fragment analyzer (Agilent Technologies).

Library preparation and RNA sequencing

RNAseq libraries were prepared with the SMART-seq v4 PLUS kit (Takara Bio Inc.) from 9.5ng of total RNA (for sample 2_UN_DonorB_3 only 3.6 ng were available) using a unique dual indexing strategy. Libraries were quantified by a fluorometric method (QubIT, Life Technologies) and their quality assessed on a Fragment Analyzer (Agilent Technologies). Sequencing was performed on an Illumina NovaSeq 6000 for 100 cycles single read (reagent version 1.5). Sequencing data were demultiplexed using the bcl2fastq2 Conversion Software (version 2.20, Illumina).

Real time quantitative PCR (RT-qPCR)

Purified RNA was reverse-transcribed into cDNA using the High-Capacity cDNA Reverse Transcription Kit (Applied Biosystems™). cDNA was purified using the QIAquick PCR purification Kit (Qiagen) according to manufacturer's instructions. Gene expression was assessed by RT-qPCR using the SYBR green I Master (Roche) and the LightCycler system (Roche). Alternatively, RT-qPCR was conducted using SYBR Green Master Mix (Applied Biosystems) on a CFX-96 platform (BioRad). Sequences of specific primer pairs (Microsynth) for *TNF, CCL3, CCL4, MT1A, HPRT* genes are listed in Table S3.

Multiplex immunoassay and ELISA

Human or murine neutrophils were cultured in RPMI-1640 medium (Gibco) supplemented with 10% FBS (Gibco) (2.5×10^6 cells/mL) in the presence or absence of parasites at an MOI of 2 for 18h. In parallel, human neutrophils were stimulated with resiquimod (R848) (InvivoGen) at 5 μM. Cytokine concentration in the culture supernatant of human neutrophils was measured using a custom-made ProcartaPlex™ Mix & Match panel (Thermo Fisher) for the detection of 13 analytes (CCL3, CCL4, CD48, CXCL5, Fas, IL-6, CXCL8, CXCL10, M-CSF, SCGF beta, TIMP-1, TNF, VEGF-R1). Data are measured (technical triplicates) in supernatants of neutrophils independently infected with 3 different MA^R and MA^S strains, left untreated or activated with R848. The mean values represented for the infected (⊛) and uninfected (○) conditions. Only cytokine/chemokine values within the limit of quantification were considered (0.5 - 62.5 pg/mL, depending on the analyte analyzed). Acquisition was performed using a Bio-Plex™ instrument (Bio-Rad) and analyzed with Bio-Plex™ manager software (Bio-Rad). For the TLR8 inhibition experiments, human neutrophils were pre-treated for 30 min with 20 μM CU-CPT9a (InvivoGen) or vehicle, and then stimulated, or not, with parasites or R848 as previously described in the presence or absence CU-CPT9a (further diluted to 10 μM) for 18h. TNF, CCL3, CXCL1 and CXCL2 concentration in the culture supernatant of murine neutrophils was quantified by ELISA using kits from R&D systems or Invitrogen (see key resources table). CXCL8 and CCL3 concentration in the supernantant of human neutrophils was measured using ELISA kits from R&D or Invitrogen, respectively.

Transwell cell migration assays

Migration of human monocytes and human neutrophils towards supernatants from neutrophils cultured under different conditions was assessed using 24-transwell plates (Corning Costar). Monocytes or neutrophils (1×10^5) were added to the upper chambers on top of 5-μm pore or 3-μm pore membranes, respectively. Supernatants from neutrophils were placed in the lower compartment after being incubated or not with Evasin-1[29] at 2 nM, or antibodies neutralizing IL-8 (1 μg/mL, R&D) or their isotype matched antibodies (1 μg/mL, R&D). In parallel, RPMI (Gibco) at 5% BSA (ITW Reagents) in the presence or absence of fMLP (Sigma) at 0.1 μM or CCL3 (R&D) at 10 ng/mL, previously incubated or not with Evasin-1 at 2nM, were included in the lower chambers in monocyte migration experiments as technical controls. After incubation of 4 h for monocytes and 1.5 h for neutrophils, the number of cells that migrated towards the lower compartment were counted by flow cytometry based on FSC and SSC parameters using an Accuri™ flow cytometer (BD Biosciences).

ROS production by murine neutrophils

ROS production was measured by luminol-based chemiluminescence assay as previously described.[17] Briefly, neutrophils were exposed to either parasites or PMA at 5 μg/mL (Sigma) with or without DPI at 1.5 μg/mL (Sigma), as negative or positive controls, respectively. Luminol (Sigma) was added and ROS chemiluminescence was measured over time using a SpectraMax® plate reader (Molecular Devices).

In vivo injections and evasin-1 treatment

Stationary promastigotes (1×10^5) of *L. (V.) panamensis* or PBS were needle-injected intradermally in the ear of BALB/c mice. For *in vivo* depletion of CCL3, mice were treated with 10 μg of Evasin-1, which was injected intraperitoneally 2h before injection of the parasite, similarly to the strategy followed in the study by Charmoy et al.[37] As controls, mice were injected with an identical volume of PBS.

Flow cytometry analysis of ear skin cell populations

At 24 h post-infection, mice were sacrificed and ears were processed to obtain single-cell suspensions as previously described.[74] Briefly, the two dermal layers of ears were separated with forceps, homogenized, and digested using 0.2 mg/mL Liberase (Roche) for 2h at 37°C. Digested ear tissue was then filtered through 40 μm filters (Falcon). Cells were incubated with the following antibodies to detect the expression of cell surface mouse markers: anti-CD45 (30-F11) -PerCP/Cy5.5, anti-Ly6C (AL-21)-FITC, anti-Ly6G (1A8)-APC/Cy7, anti-CD11b (M1/70)-BV605, anti-CD11c (N418)-PE, anti-CD206 (C068C2)- PE/Cy7 and anti-SiglecF (E50-2440)-BUV395. Cell viability was analyzed using the Live/Dead fixable Aqua Dead Cell Stain Kit (Invitrogen). To detect intracellular TNF, ear cells were cultured for 4 h at 37°C in the presence of 1 μg/mL GolgiPlug (BD Bioscience). Cells were stained for surface markers and Live/Dead dye, and fixed and permeabilized with eBioscience™ Fixation and Permeabilization Buffer Set. TNF was detected upon staining with anti-TNF (MP6-XT22)-APC antibody (BD Biosciences). Cells were analyzed using LSR-Fortessa (BD Bioscience) and FlowJo software (BD).

QUANTIFICATION AND STATISTICAL ANALYSIS

RNA-seq data processing

Raw fastq reads were processed by: 1) trimming adapters and low-quality ends with Cutadapt (v. 2.5[65]); 2) removing ribosomal RNA sequences with fastq_screen (v. 0.11.1[66]) and 3) filtering out low complexity reads using reaper (v. 15-065[67]). Next, reads were aligned against *Homo sapiens* genome (build GRCh38) using STAR (v. 2.5.3a[68]). Gene counts were obtained with htseq-count (v. 0.9.1) using Human Ensembl 102 gene annotation. The quality of the RNA-Seq data alignment was evaluated using RSeQC (v. 2.3.7[73]). Gene counts matrix was imported into the R software (v. 4.1.1). Genes characterized by low expression counts were excluded based on the criterion of having at least 1 count per million (cpm) in a minimum of 1 sample. The library sizes were normalized using TMM procedure and log-transformed into counts per million or CPM (EdgeR package v. 3.34.1). Normalized counts were corrected for donor pairing using removeBatchEffect function from limma package and used for generating a PCA plot.

Differential expression analysis

Differential expression was computed with limma-trend approach[70] by including all samples in a single linear model. The donor pairing coefficient was included in the model. The correlation between intra-donor *Leishmania* infection replicates was estimated using duplicateCorrelation function and integrated into the linear model fitting process. Moderated t-test was used for each contrast and the adjusted p-value was computed by the Benjamini-Hochberg method, controlling for false discovery rate (FDR).

Clustering and heatmap of variable genes

Heatmaps including hierarchical clustering were generated by pheatmap R package (v 1.0.12) using correlation distance and cutree function for defining clusters.

Gene ontology and gene set enrichment analyses

Over-representation analysis (ORA) of significant genes in pathways was performed on GO terms - biological process (GO BP) using enrichGO function (R package clusterProfiler[73]). P-values to represent the enrichment of GO terms were calculated with a one-sided Fisher test and adjusted for multiple testing by the Benjamini-Hochberg method, which controls the false discovery rate (FDR). Analysis was performed for the upregulated and downregulated gene lists separately and enriched GO terms were simplified to remove redundant GO terms using simplify function with the parameter cutoff=0.5. cnetplot function (enrichplot package v1.20.0) was employed for generating network figures.

Gene set enrichment analysis or GSEA was performed using the R Bioconductor package ClusterProfiler (fgsea function). The input for GSEA consisted of a ranked gene list by the t statistic. The method calculates an enrichment score for each gene set. This score signifies the extent to which a gene set is concentrated at either the upper or lower end of the ranked gene list. The p-value of the enrichment score is calculated using a permutation test and FDR is reported to account for multiple hypothesis testing. GSEA of differentially expressed genes against MSigDB was performed using the Molecular Signatures Database (Human MSigDB v2022. 1. Hs).[22,23]

Mapping of gene modules onto scRNA-Seq data

Our defined neutrophil gene modules defined by bulk RNA-Seq were mapped onto the UMAP plot (Figure 6A) from Montaldo et al.[26] scRNA-seq data (E-MTAB-11188 and Seurat object provided by authors). The Seurat function AddModuleScore (V4.3.0) was used to calculate the average expression levels of each module at a single cell level, subtracted by the aggregated expression of randomly selected control feature sets.[75] UMAP plots were generated for each module and each cell colored based on the computed scores. Dotplots of the 10 most expressed genes of each module were created and colored by the average expression per gene.

Relative quantification of RT-qPCR data

Relative gene expression was performed using the $2^{-\Delta\Delta CT}$ method, calculating the first ΔCT as the difference in threshold cycle (CT) between the target genes and the housekeeping gene hypoxanthine phosphoribosyl transferase (*HPRT*). For the calculation of $\Delta\Delta CT$, uninfected samples were considered as the reference condition to quantify *TNF*, *CCL3* and *CCL4* gene expression, while MA^S-infected conditions were used as reference for *MT1A* due to the minimal, often undetectable, expression of this gene in uninfected samples.

Statistical analysis

The rest of numerical data were analyzed with GraphPad Prism version 9.5.1 using statistical test noted within the corresponding figure captions. Unless otherwise stated in the figure legends, P values were annotated as: * < 0.05, ** < 0.01, *** < 0.001, and **** < 0.0001.